Photonics & Plasmonics with Metamaterials

Carlos **A**lberto **A**ragão **de Carvalho Fº**
DGDNTM & IF-UFRJ

Palestra de Abertura da EPG/UERJ
14/08/2017

February 2001
“100 years of quantum misteries”

------->

“In a few years, all the great physical constants will have been approximately estimated, and … the only occupation which will then be left to the men of science will be to carry these measurements to another place of decimals.” As we enter the 21st century amid much brouhaha about past achievements, this sentiment may sound familiar. Yet the quote is from James Clerk Maxwell and dates from his 1871 University of Cambridge inaugural lecture expressing the mood prevalent at the time (albeit a mood he disagreed with). Three decades later, on December 14, 1900, Max Planck announced his formula for the blackbody spectrum, the first shot of the quantum revolution.

This article reviews the first 100 years of quantum mechanics, with particular focus on its mysterious side, culminating in the ongoing debate about its consequences for issues ranging from quantum computation to consciousness, parallel universes and the very nature of physical reality. We virtually ignore the astonishing range of scientific and practical applications that quantum mechanics undergirds: today an estimated 30 percent of the U.S. gross national product is based on inventions made possible by quantum mechanics, from semiconductors in computer chips to lasers in compact-disc players, magnetic resonance imaging in hospitals, and much more.

In 1871 scientists had good reason for their optimism. Classical mechanics and electrodynamics had powered the industrial revolution, and it appeared as though

------->

electronics x photonics

PHOTONICS

The photonic crystal is the working currency of photonics. It is a regular structure that offers propagating photons a periodic variation in refraction index. That periodicity can range in size from centimeters for some applications, down to tens of nanometers for others.

Photonic crystals: putting a new twist on light, J. D. Joannopoulos, P. R. Villeneuve, and S. Fan, Nature 386, 143 (1997)

Photonic crystals are materials patterned with, e.g., a periodicity in the dielectric constant, which can create a range of «forbidden» frequencies called a photonic bandgap. Photons with energies lying in the bandgap cannot propagate through the medium. This provides the opportunity to shape and mould the flow of light for photonic information technology.

- **imminent technological revolutions in signal processing, communications, computing, astrophysics, biology, medicine, etc.**

Manipulating the flow of light with photonic crystals, Peter Vukusic Physics Today, October 2006, p. 82

Microfabricated

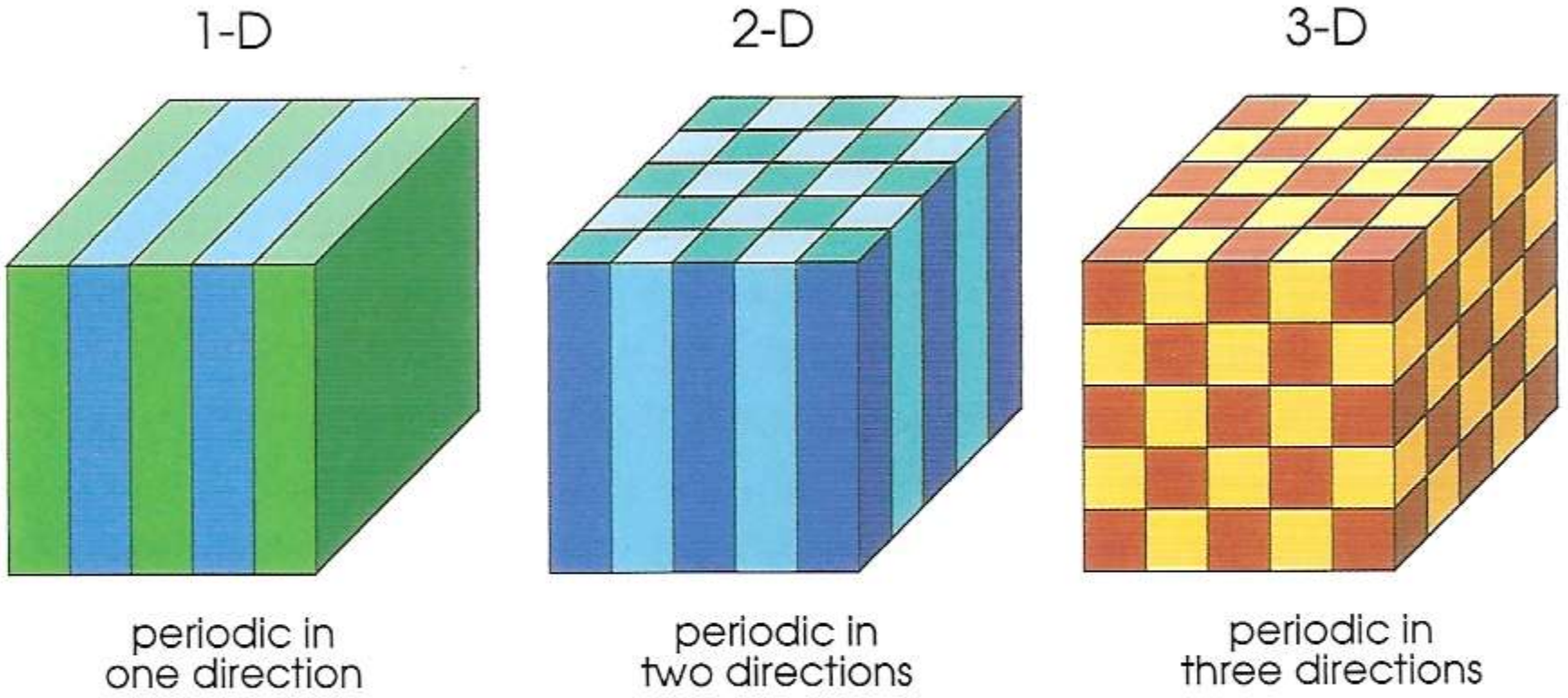

Figure 1 Simple examples of one-, two-, and three-dimensional photonic crystals. The different colors represent materials with different dielectric constants. The defining feature of a photonic crystal is the periodicity of dielectric material along one or more axes.

Photonic crystals, by J D Joannopoulos et al, Princeton U. Press (2008)

Microfabricated

Defects: Localization and waveguiding properties

cavity

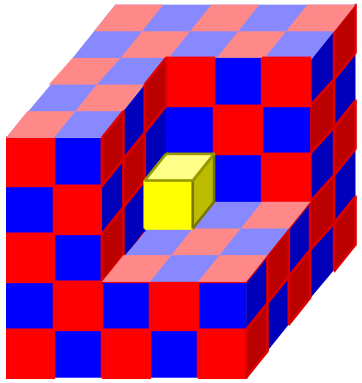

waveguide

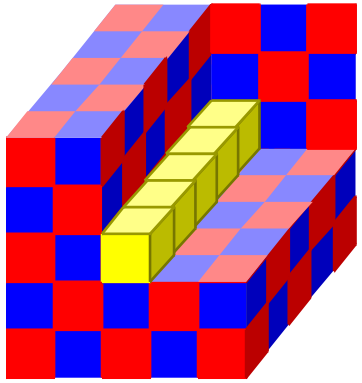

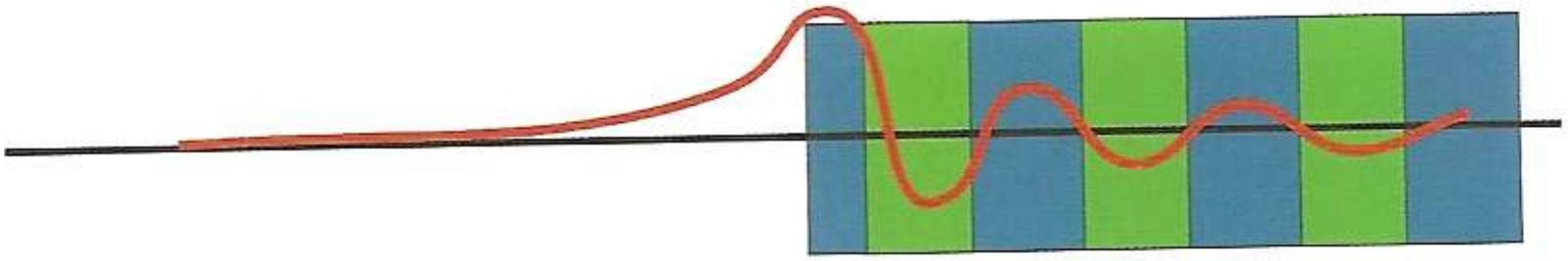

Figure 12 The electric field strength associated with a localized mode at the surface of a multilayer film.

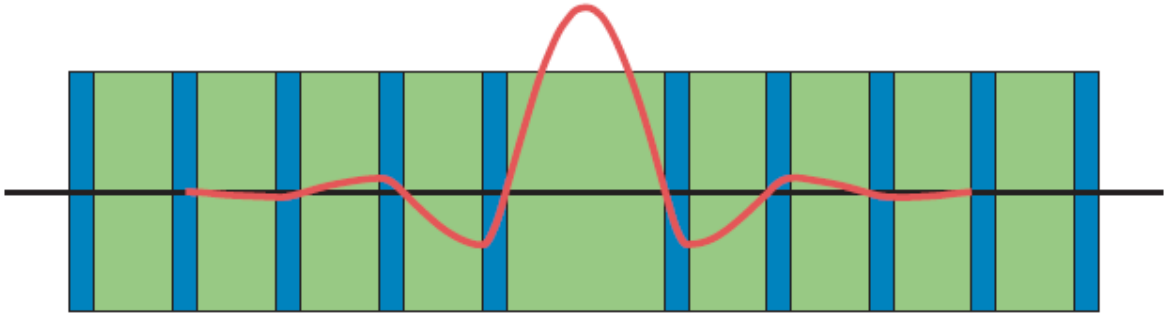

Figure 11: A defect in a multilayer film, formed by doubling the thickness of a single *low-ε* layer in the structure of figure 5. Note that this can be considered to be an interface between two perfect multilayer films. The red curve is the electric-field strength of the defect state associated with this structure (for on-axis propagation).

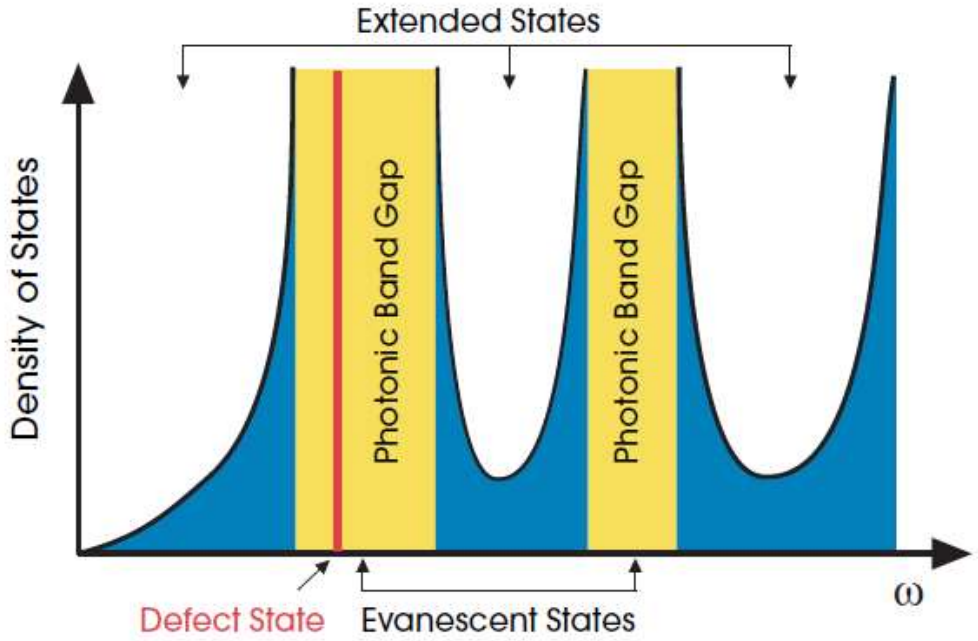

Figure 12: The division of frequency space into extended and evanescent states. In this sketch, the **density of states** (the number of allowed modes per unit frequency) is zero in the band gaps of the crystal (yellow). Modes are allowed to exist in these regions only if they are evanescent, and only if the translational symmetry is broken by a defect. Such a mode is shown in red.

Table 1

	Quantum Mechanics	*Electrodynamics*
Field	$\Psi(\mathbf{r},t) = \Psi(\mathbf{r})e^{-iEt/\hbar}$	$\mathbf{H}(\mathbf{r},t) = \mathbf{H}(\mathbf{r})e^{-i\omega t}$
Eigenvalue problem	$\hat{H}\Psi = E\Psi$	$\hat{\Theta}\mathbf{H} = \left(\frac{\omega}{c}\right)^2 \mathbf{H}$
Hermitian operator	$\hat{H} = -\frac{\hbar^2}{2m}\nabla^2 + V(\mathbf{r})$	$\hat{\Theta} = \nabla \times \frac{1}{\varepsilon(\mathbf{r})}\nabla \times$

Comparison of quantum mechanics and electrodynamics.

Table 1

	Quantum Mechanics	*Electrodynamics*
Discrete translational symmetry	$V(\mathbf{r}) = V(\mathbf{r}+\mathbf{R})$	$\varepsilon(\mathbf{r}) = \varepsilon(\mathbf{r}+\mathbf{R})$
Commutation relationships	$[\hat{H}, \hat{T}_\mathbf{R}] = 0$	$[\hat{\Theta}, \hat{T}_\mathbf{R}] = 0$
Bloch's theorem	$\Psi_{\mathbf{k}n}(\mathbf{r}) = u_{\mathbf{k}n}(\mathbf{r})e^{i\mathbf{k}\cdot\mathbf{r}}$	$\mathbf{H}_{\mathbf{k}n}(\mathbf{r}) = \mathbf{u}_{\mathbf{k}n}(\mathbf{r})e^{i\mathbf{k}\cdot\mathbf{r}}$

Quantum mechanics vs. electrodynamics in periodic systems.

Photonic crystals, by J D Joannopoulos et al, Princeton U. Press (2008)

electronics x photonics

GaAs:
semiconductor

electronic band gap

device applications

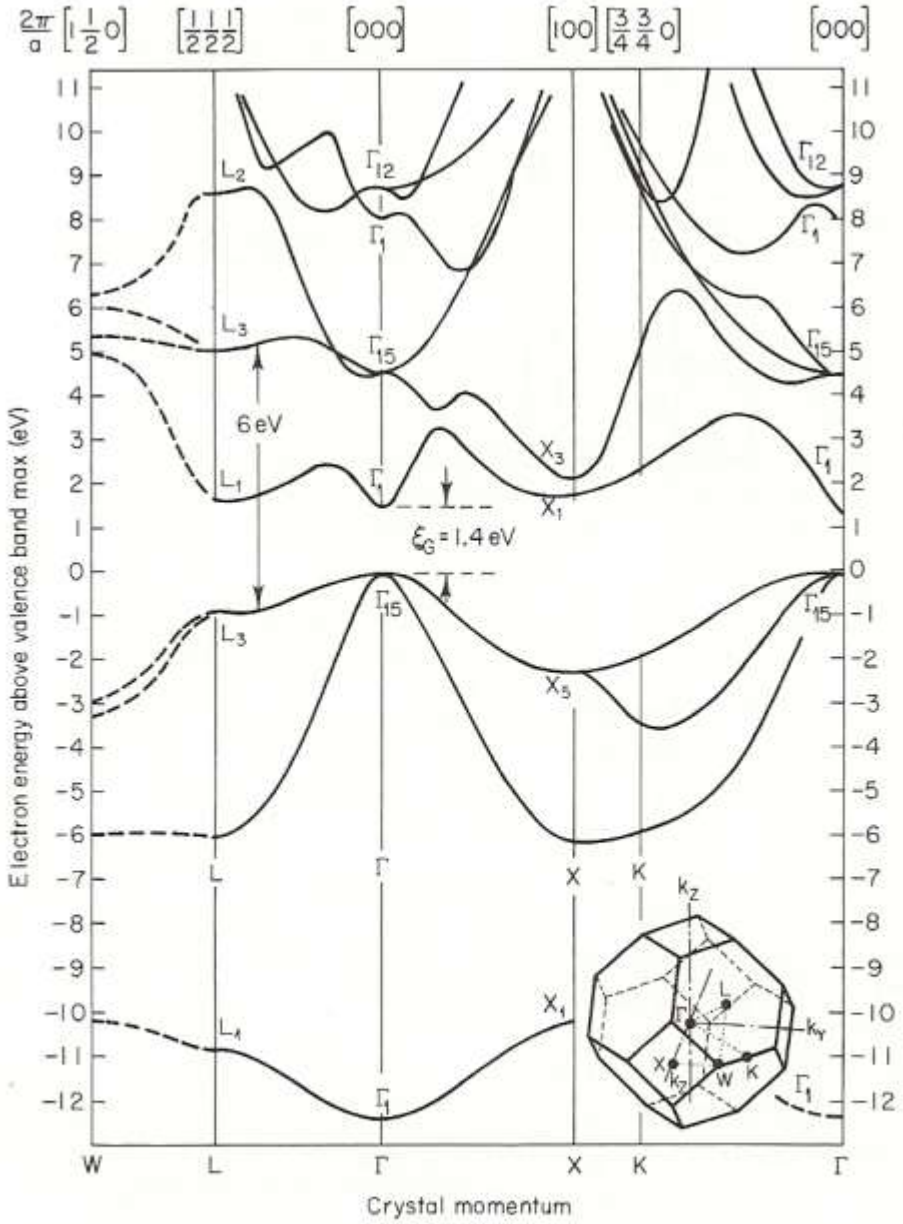

Fig. 1.5 Energy band diagram for GaAs. Compare this diagram with Fig. 1.1 to see the effect of the finite periodic crystal potential in GaAs. [Based on M. L. Cohen and T. K. Bergstresser, *Phys. Rev.* **141**, 789 (1966).]

Photonic crystals: photonic band gap device applications

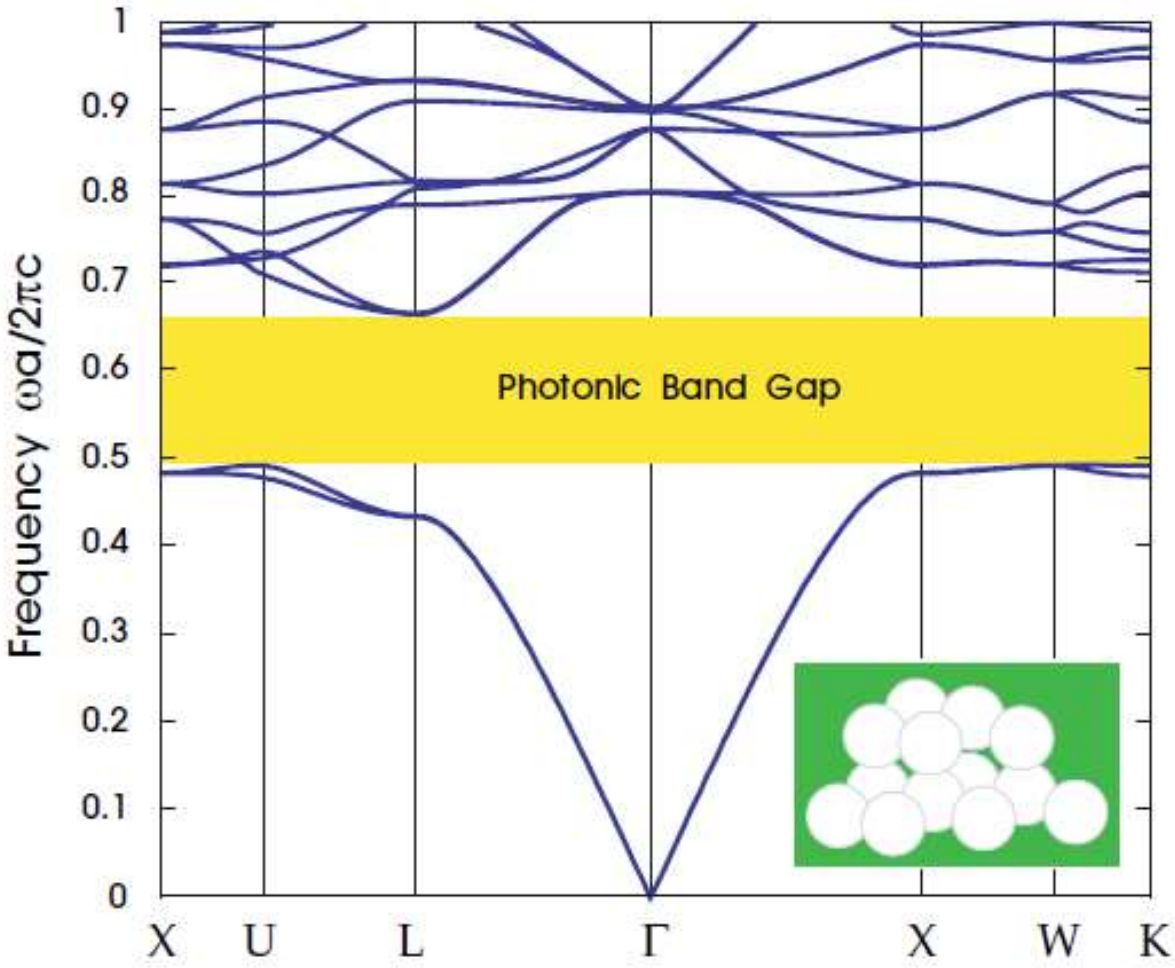

Figure 3: The photonic band structure for the lowest bands of a diamond lattice of air spheres in a high dielectric ($\varepsilon = 13$) material (inset). A complete photonic band gap is shown in yellow. The wave vector varies across the irreducible Brillouin zone between the labelled high-symmetry points; see appendix B for a discussion of the Brillouin zone of an fcc lattice.

- **A Plasmon is a quasiparticle resulting from the quantization of plasma oscillations just as photons and phonons are quantizations of light and mechanical vibrations, respectively.**

$$\varepsilon(q=0,\omega)=1-\frac{\omega_p^2}{\omega^2}$$

RPA-electron gas
Drude model

plasmon freq.:

$$\omega_p^2=\frac{4\pi ne^2}{m}$$

WHAT IS A PLASMON POLARITON?

- **Plasmons can couple with photons to create plasmon-polariton quasiparticles.**

April 2007: Plasmonics

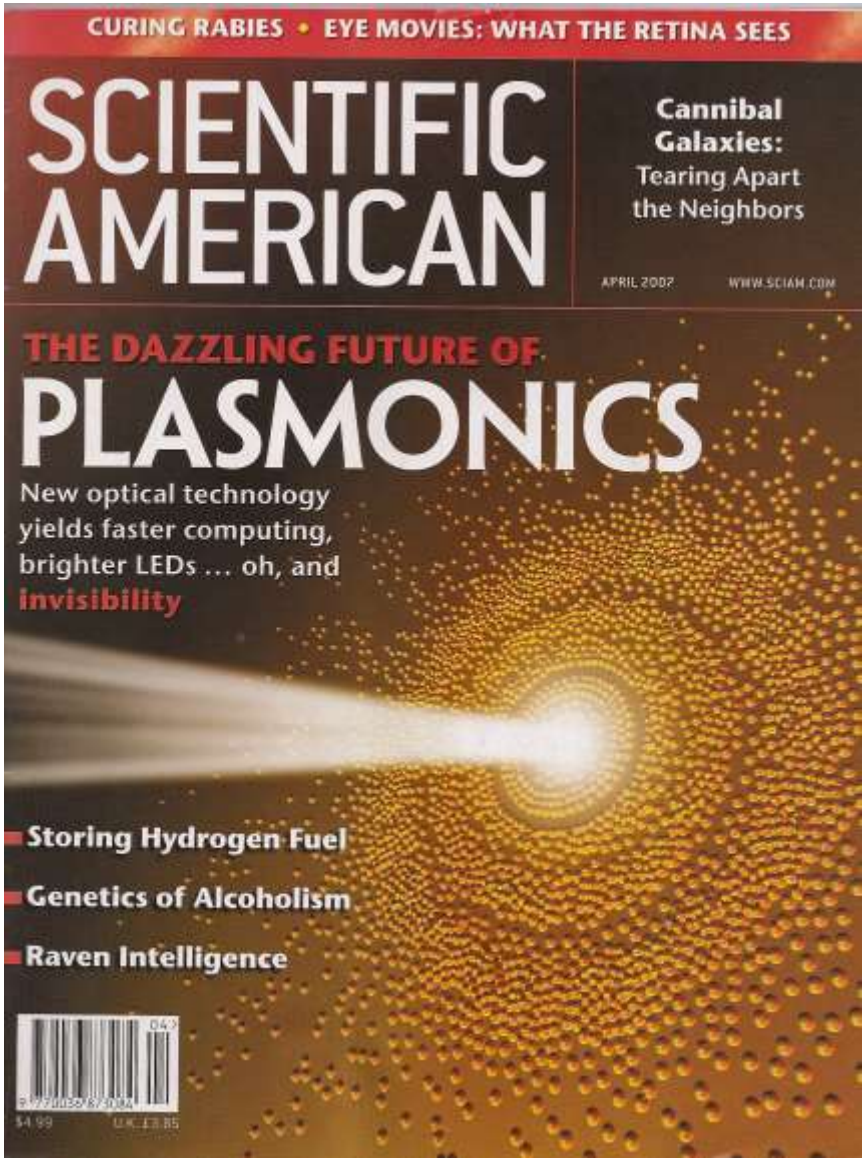

Feb 2011: Illuminating nanoplasmonics

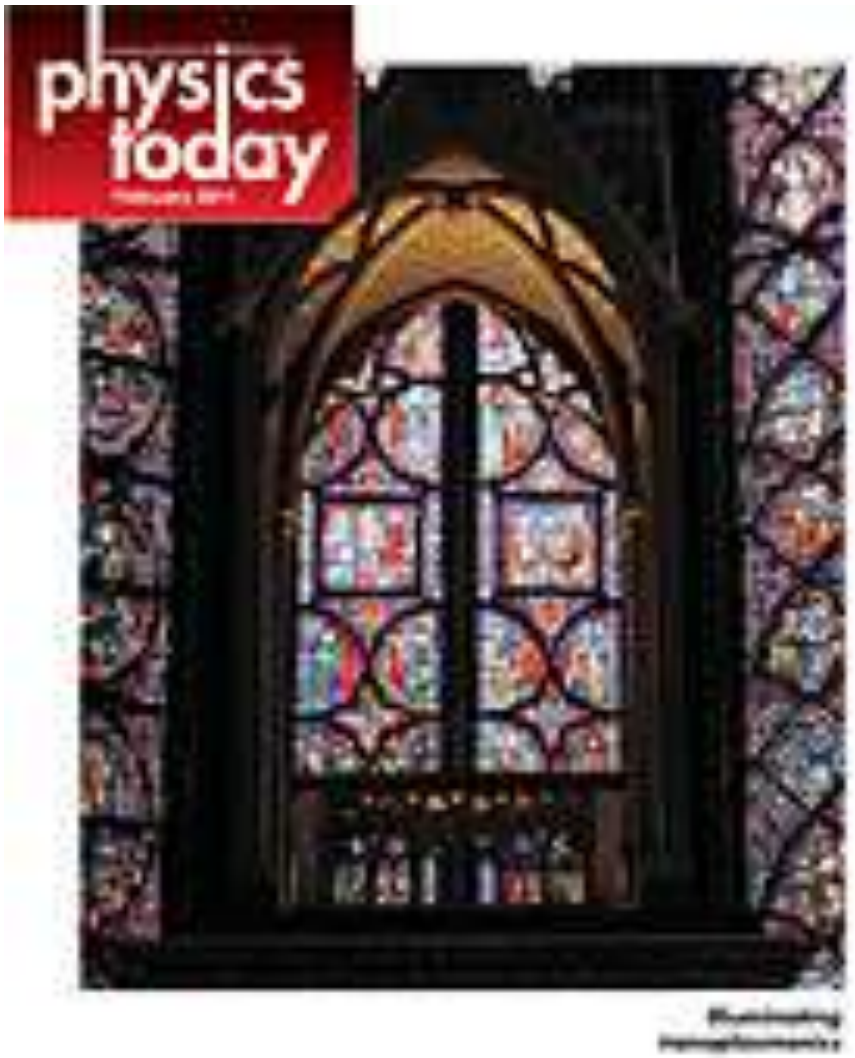

Nanoplasmonics: The physics behind the applications, M. I. Stockman, Feb 2011, Phys. Today, p. 39

Overview/*Plasmonics*

- Researchers have discovered that they can squeeze optical signals into minuscule wires by using light to produce electron density waves called plasmons.
- Plasmonic circuits could help the designers of computer chips build fast interconnects that could move large amounts of data across a chip. Plasmonic components might also improve the resolution of microscopes, the efficiency of light-emitting diodes, and the sensitivity of chemical and biological detectors.
- Some scientists have even speculated that plasmonic materials could alter the electromagnetic field around an object to such an extent that it would become invisible.

Scientific American, April 2007

Metamaterials

(negative index structures, left-handed materials)

μετα = beyond

SOVIET PHYSICS USPEKHI VOLUME 10, NUMBER 4 JANUARY-FEBRUARY 1968

538.30

THE ELECTRODYNAMICS OF SUBSTANCES WITH SIMULTANEOUSLY NEGATIVE VALUES OF ε AND μ

V. G. VESELAGO

P. N. Lebedev Physics Institute, Academy of Sciences, U.S.S.R.

Usp. Fiz. Nauk 92, 517–526 (July, 1964)

$$n = \sqrt{\mu}\sqrt{\epsilon}$$

ε<0 & μ<0 imply n<0
negative index of refraction

Split Ring Resonators

The three connected metallic rods, which make the U-type SRR structure, act as a nano-inductor, while the gap between the ends of the U-shape act like a nano-capacitor. This nano-LC circuit acts as an LC resonator with a resonance frequency at optical frequencies. More important, the typical size of these resonant inclusions is approximately 10 times smaller than the vacuum wavelength of the light at the resonance frequency. The electromagnetic properties of such optical-scale subwavelength structures can then be evaluated by using an effective medium approximation.

SRR structures: Photo of nanoscale split ring resonator structures fabricated in Bilkent University.

Conventional materials:
properties derive from their constituent *atoms*

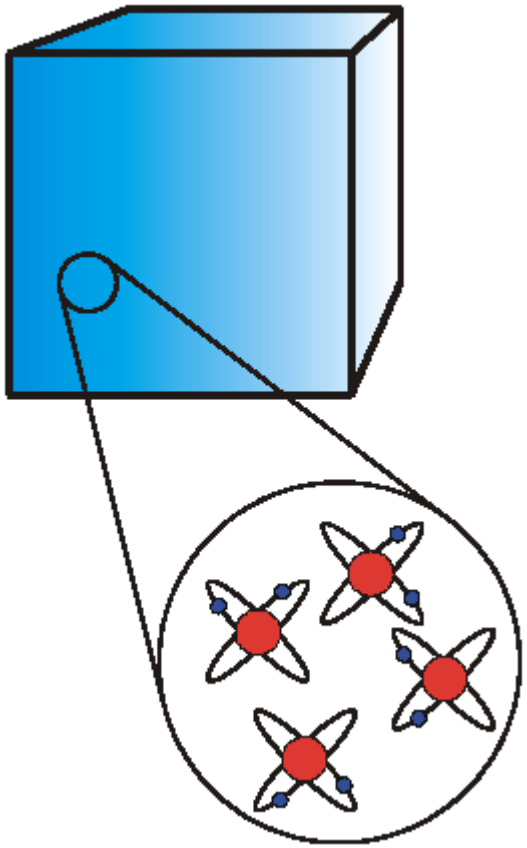

Metamaterials: properties derive from their constituent units; these units may be engineered

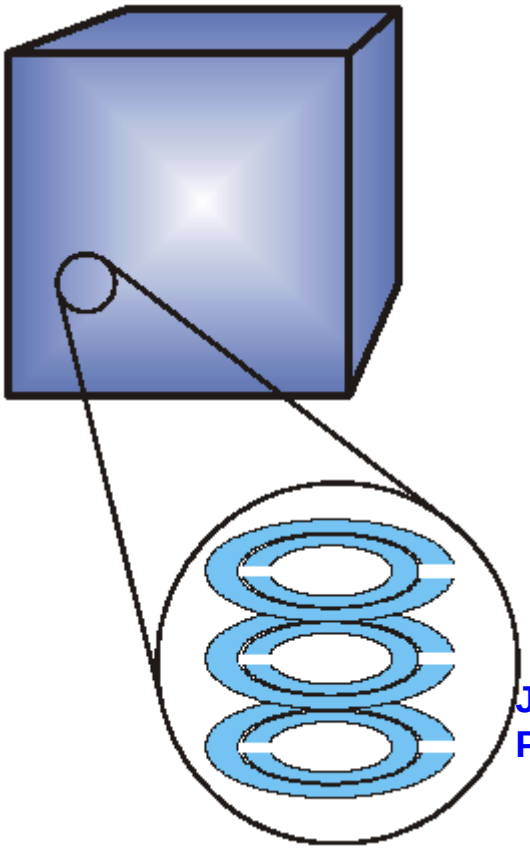

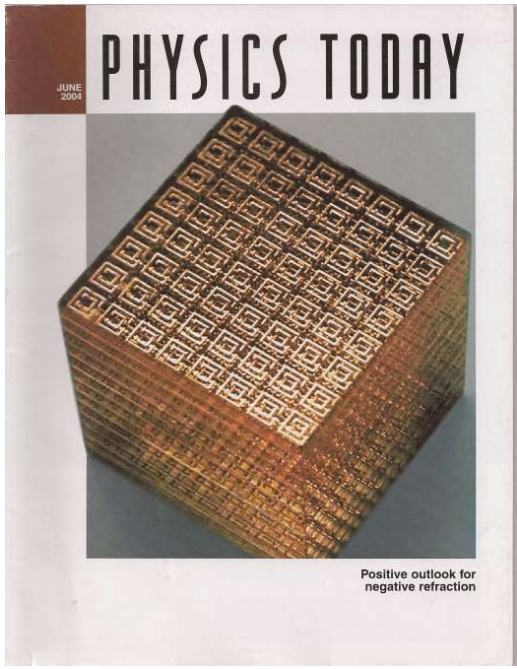

J. Pendry and D. Smith, Phys. Today, June 2004, p.37

A Roadmap for Metamaterials, N. I. Zheludev
OPN Optics & Photonics News March 2011 | 31

Conceptually replace the inhomogeneous composite by a continuous material described by material parameters ε and μ.

SCIENCE By Nikolay I. Zheludev[1,2] 29 MAY 2015 • VOL 348 ISSUE 6238 973

Obtaining optical properties on demand

Reconfigurable metamaterials provide a flexible platform for nanophotonic technology

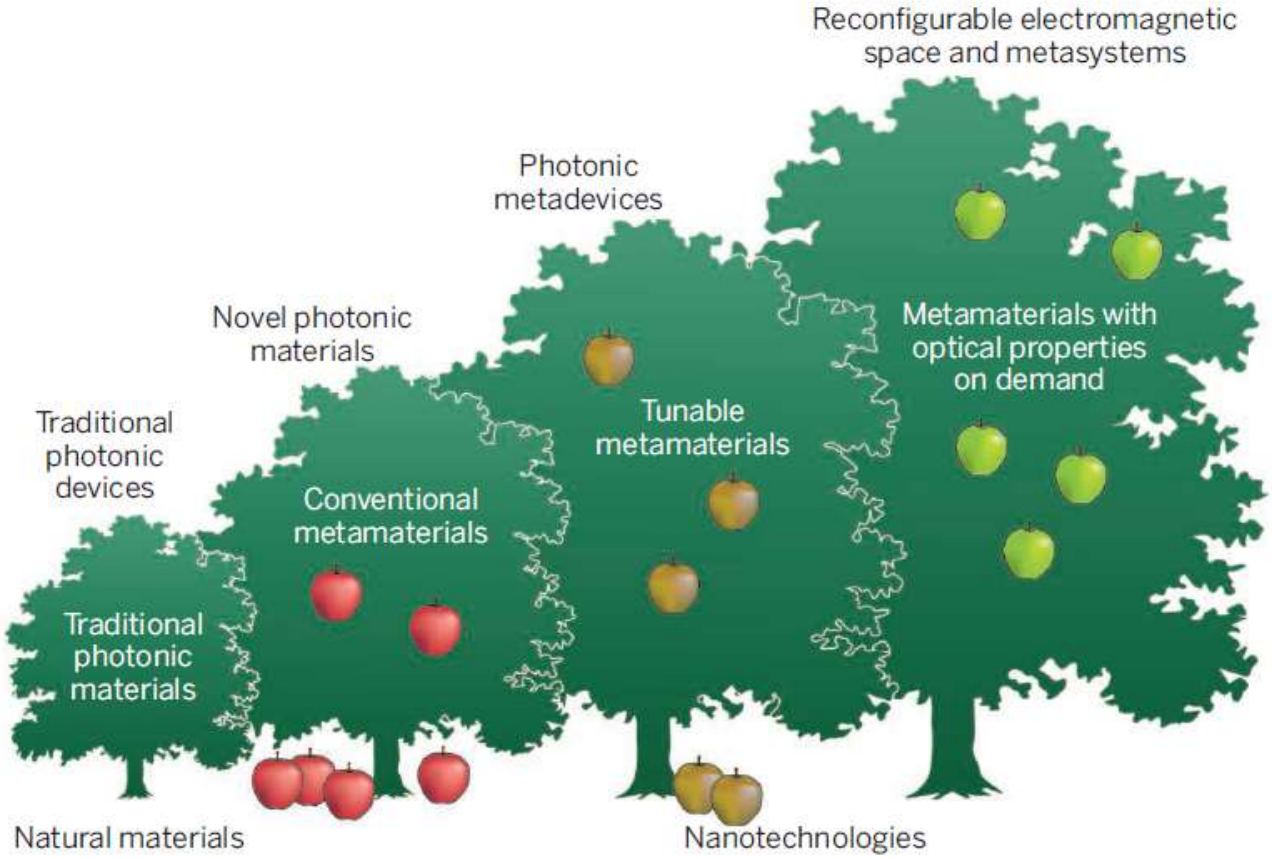

Mighty metamaterials forest. Metamaterials were first developed as artificial media structured on a size scale smaller than the wavelength of external stimuli. They showed novel, now well-understood electromagnetic properties, such as negative index of refraction or optical magnetism, allowing devices such as optical cloaks and superresolution lenses. Tunable, nonlinear, switchable, gain-assisted, sensor, and quantum metamaterials appeared and increased the potential for device integration of metamaterial technology. The coming challenge is to develop metamaterials with on-demand optical properties that may be independently controlled for every individual metamolecule of the nanostructure.

Advances in metamaterials

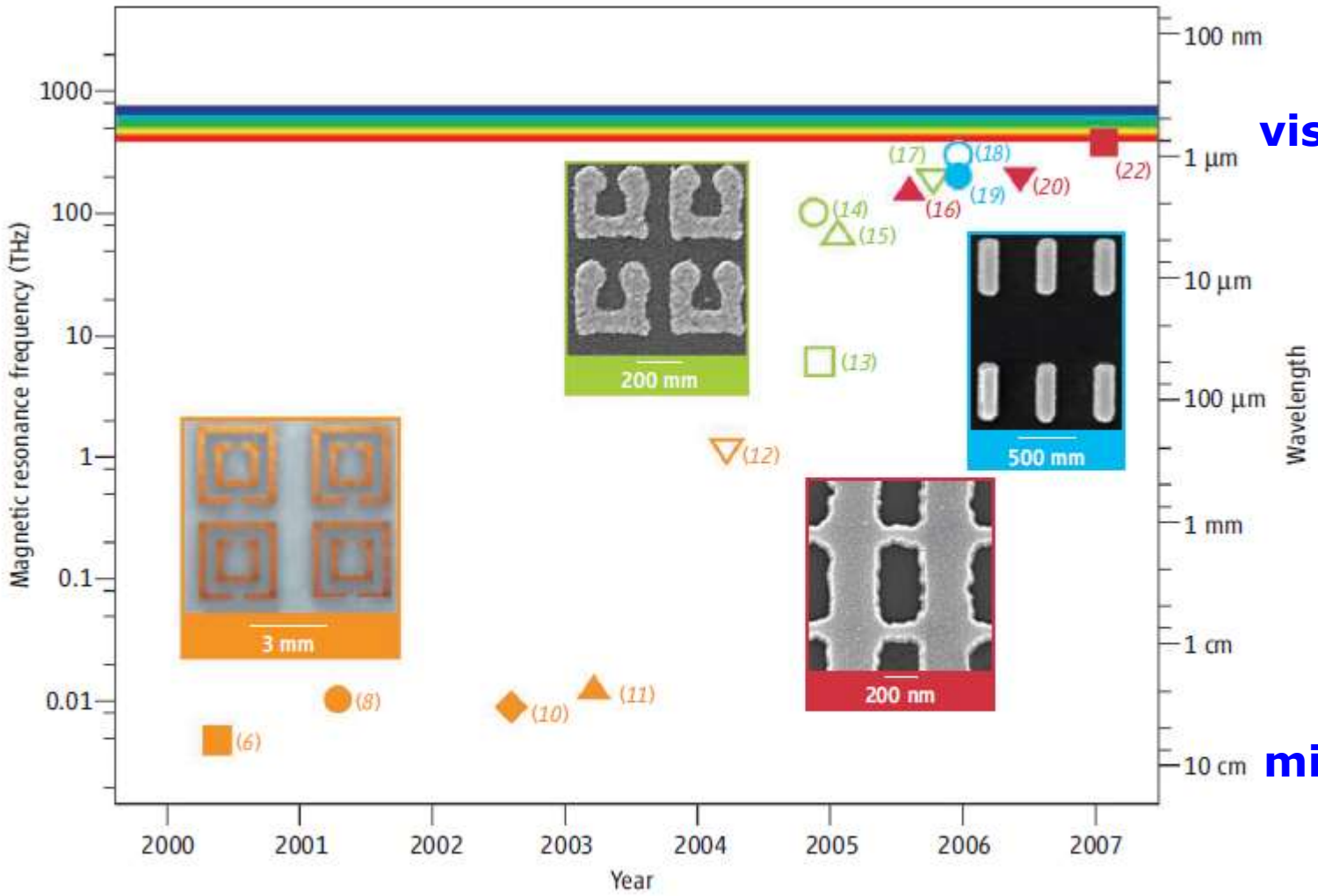

Advances in metamaterials. The solid symbols denote $n < 0$; the open symbols denote $\mu < 0$. Orange: data from structures based on the double split-ring resonator (SRR); green: data from U-shaped SRRs; blue: data from pairs of metallic nanorods; red: data from the "fishnet" structure. The four insets give pictures of fabricated structures in different frequency regions.

Science **315**, 47 (2007)

Costas M. Soukoulis, Stefan Linden, Martin Wegener

Metamaterials: various possible dispersive responses

1. $$\varepsilon_{d_0}(\omega) = \varepsilon_{10} - \frac{\alpha}{\omega^2}, \mu_{d_0}(\omega) = \mu_{10} - \frac{\beta}{\omega^2}$$

2. $$\varepsilon_{d_0} \approx (C_0 - \frac{1}{(2\pi f)^2 L d_0})/(\varepsilon_0 p)$$
$$\mu_{d_0} \approx p(L_0 - \frac{1}{(2\pi f)^2 C d_0})/\mu_0$$

3. $$\epsilon_b(\omega) = \epsilon_0 - \frac{\omega_e^2}{\omega(\omega + i\gamma_e)}, \quad \mu_b(\omega) = \mu_0 - \frac{\omega_m^2}{\omega(\omega + i\gamma_m)}$$

4. $$\epsilon(\omega) = 1 - \frac{\omega_p^2}{\omega^2}, \quad \mu(\omega) = 1 - \frac{F\omega^2}{(\omega^2 - \omega_r^2)},$$

5. $$\varepsilon(\omega) = 1 - \frac{\omega_p^2 - \omega_0^2}{\omega^2 - \omega_0^2 + i\omega\Gamma}, \quad \mu(\omega) = 1 - \frac{F\omega^2}{\omega^2 - \omega_0^2 + i\omega\Gamma}.$$

etc

Metamaterials
(negative index structures, left-handed materials)

V. M. Shalaev et al, Optics Lett. 30, 3356 (2005)
Negative index of refraction in optical metamaterials

Costa M. Soukoulis et al, Science 315, 47 (2007)
Negative refractive index at optical wavelengths

S. Xiao et al, and V. M. Shalaev, Nature 466, 5 August 2010
Loss-free and active optical negative-index metamaterials

study demonstrates the possibility of fabricating an optical negative-index metamaterial that is not limited by the inherent loss in its metal constituent.

L. H. Zhang et al, Eur. Phys. J. B77, 1-5 (2010)
Experimental study on multichannel-based quasi-1D photonic crystals containing negative-index materials

$$\varepsilon_{d_0}(\omega) = \varepsilon_{10} - \frac{\alpha}{\omega^2}, \mu_{d_0}(\omega) = \mu_{10} - \frac{\beta}{\omega^2}$$

June 2004

“Positive outlook for negative refraction”

To form an artificial material, we start with a collection of repeated elements designed to have a strong response to applied electromagnetic fields. As long as the size and spacing of the elements are much smaller than the electromagnetic wavelengths of interest, incident radiation cannot distinguish the collection of elements from a homogeneous material. We can thus conceptually replace the inhomogeneous composite by a continuous material described by material parameters ε and μ.

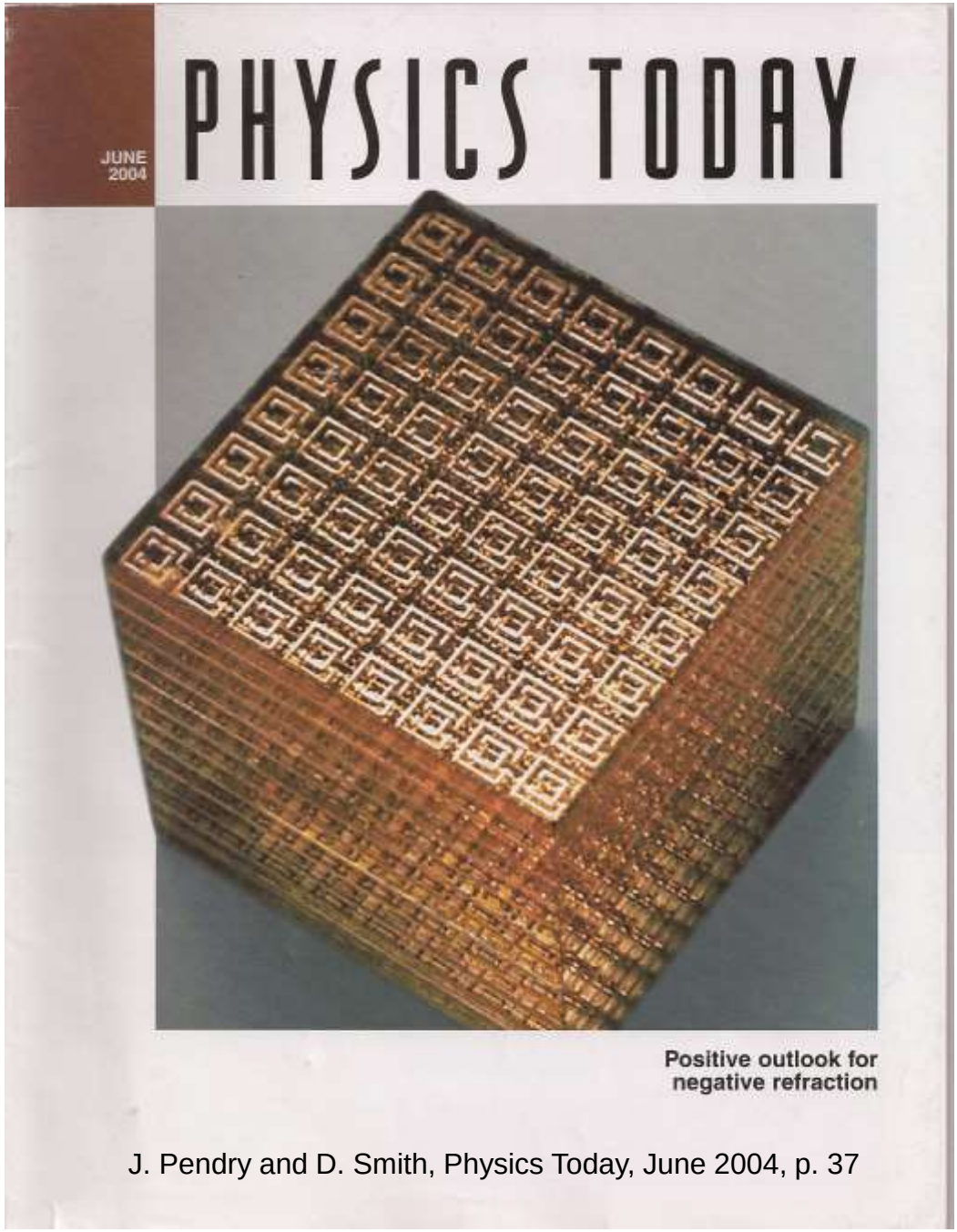

J. Pendry and D. Smith, Physics Today, June 2004, p. 37

February 2007

“Invisibility by design”

To make something invisible is to make it seem transparent. The nested fiberglass cylinders pictured here, embossed with hundreds of split copper rings, do just that—at least in the microwave regime. The trick lies in the geometry of the split rings. Collectively, they deflect microwaves around the innermost cylinder and return the waves to their original paths on the other side, hiding whatever lies inside.

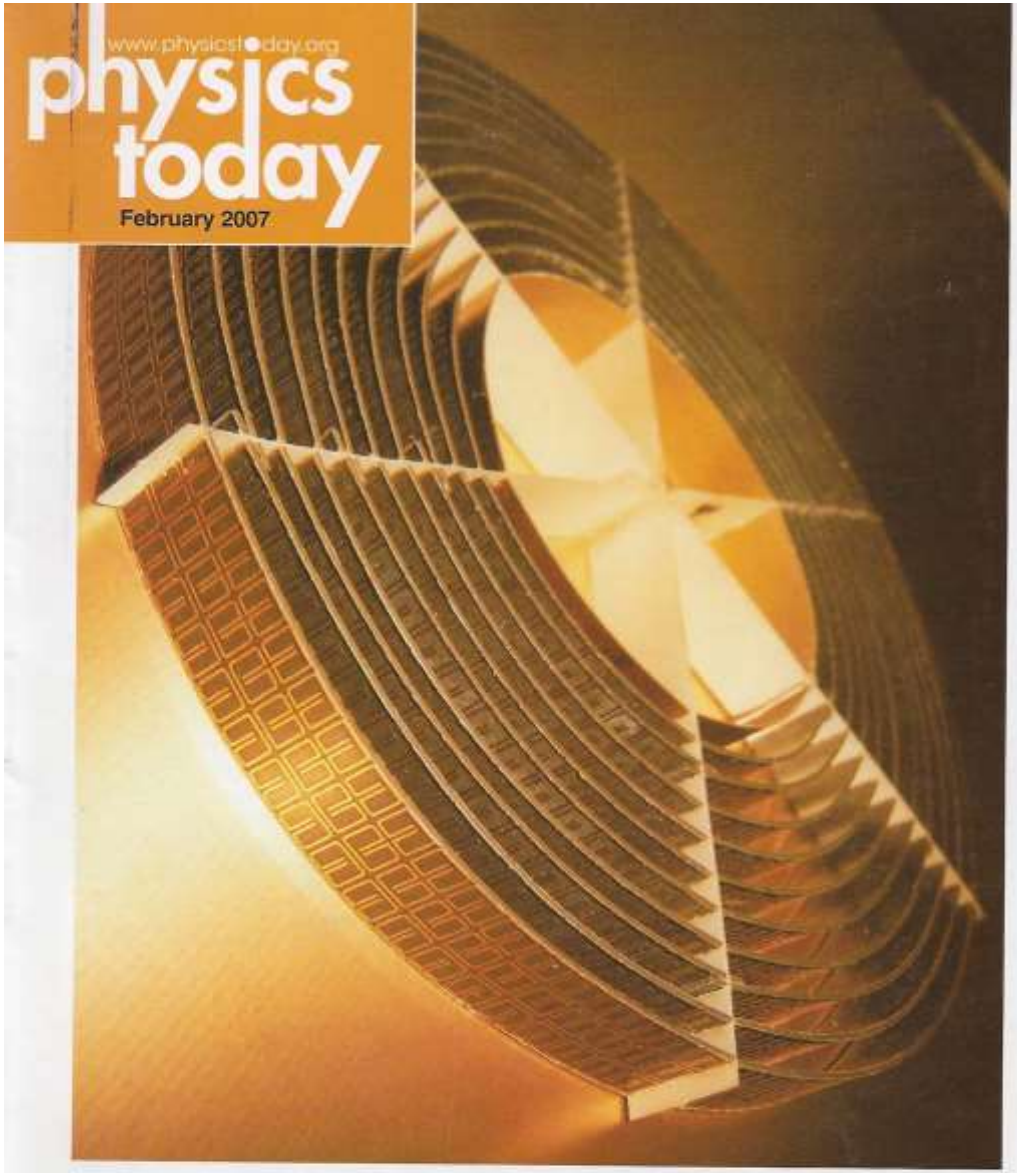

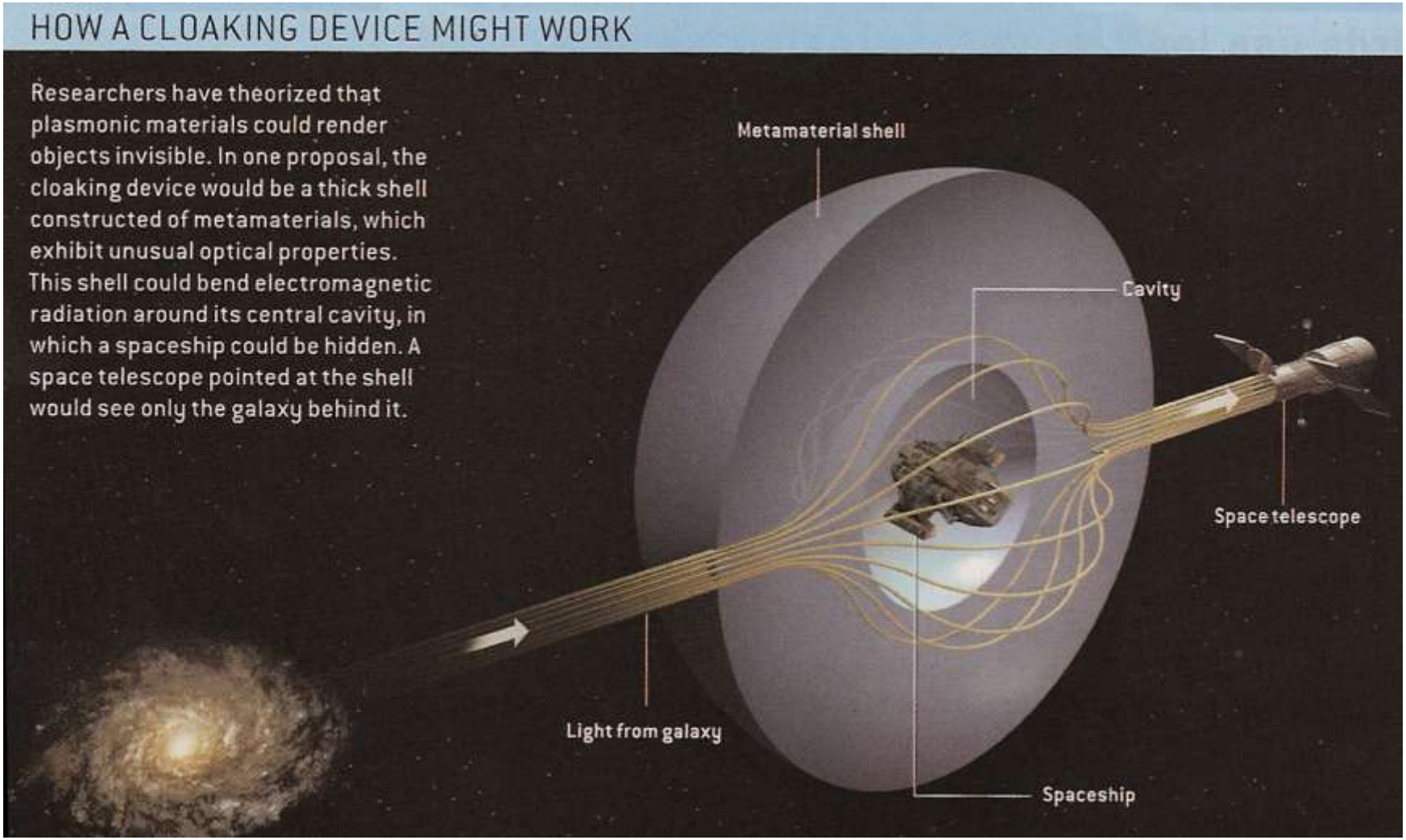

Scientific American, April 2007

Metamaterial Electromagnetic Cloak at Microwave Frequencies

D. Schurig,[1] J. J. Mock,[1] B. J. Justice,[1] S. A. Cummer,[1] J. B. Pendry,[2] A. F. Starr,[3] D. R. Smith[1]*

A recently published theory has suggested that a cloak of invisibility is in principle possible, at least over a narrow frequency band. We describe here the first practical realization of such a cloak; in our demonstration, a copper cylinder was "hidden" inside a cloak constructed according to the previous theoretical prescription. The cloak was constructed with the use of artificially structured metamaterials, designed for operation over a band of microwave frequencies. The cloak decreased scattering from the hidden object while at the same time reducing its shadow, so that the cloak and object combined began to resemble empty space.

Three-Dimensional Invisibility Cloak at Optical Wavelengths

Tolga Ergin,[1,2]*† Nicolas Stenger,[1,2]* Patrice Brenner,[2] John B. Pendry,[3] Martin Wegener[1,2,4]

We have designed and realized a three-dimensional invisibility-cloaking structure operating at optical wavelengths based on transformation optics. Our blueprint uses a woodpile photonic crystal with a tailored polymer filling fraction to hide a bump in a gold reflector. We fabricated structures and controls by direct laser writing and characterized them by simultaneous high–numerical-aperture, far-field optical microscopy and spectroscopy. A cloaking operation with a large bandwidth of unpolarized light from 1.4 to 2.7 micrometers in wavelength is demonstrated for viewing angles up to 60°.

Applications

- Antennas
- Perfect lenses
- Photonic crystals (already discussed)
- Sensors

1D Photonic Crystals

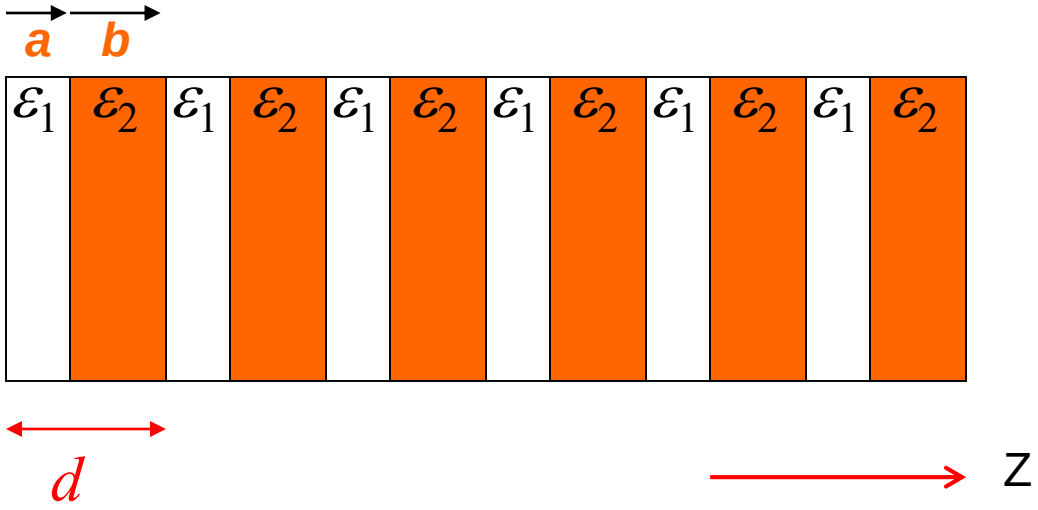

$$\varepsilon(z) = \varepsilon(z+d)$$

in-plane linearly polarized electromagnetic field of the form $\vec{E}(z,t) = E(z)e^{-i\omega t}\hat{x}$

Maxwell's equations

A monochromatic...

$$\nabla \times (\nabla \times \mathbf{E}) - \mu(\mathbf{r})\varepsilon(\mathbf{r})(\frac{\omega}{c})^2\mathbf{E} - \frac{\nabla\mu(\mathbf{r})}{\mu(\mathbf{r})} \times (\nabla \times \mathbf{E}) = 0$$

...linear polarized plane wave

$$\frac{d}{dz}[\frac{1}{n(z)Z(z)}\frac{dE(z)}{dz}] = -\frac{n(z)}{Z(z)}\frac{\omega^2}{c^2}E(z)$$

...with

$$n(z) = \sqrt{\epsilon(z)}\sqrt{\mu(z)} \text{ and } Z(z) = \sqrt{\mu(z)}/\sqrt{\epsilon(z)}$$

Transfer Matrix technique

The electric field is continuous everywhere

$$\psi(z) = \begin{pmatrix} E(z) \\ \frac{1}{nZ}\frac{dE}{dz} \end{pmatrix}$$

$$\psi(z) = M_i(z - z_0)\,\psi(z_0)$$

the transfer matrix

$$M_i(z) = \begin{pmatrix} \cos\left(\frac{\omega|n_i|}{c}z\right) & \frac{n_i}{|n_i|}\frac{cZ_i}{\omega}\sin\left(\frac{\omega|n_i|}{c}z\right) \\ -\frac{|n_i|}{n_i}\frac{\omega}{cZ_i}\sin\left(\frac{\omega|n_i|}{c}z\right) & \cos\left(\frac{\omega|n_i|}{c}z\right) \end{pmatrix}$$

$$Z(z) = \sqrt{\mu(z)}/\sqrt{\epsilon(z)}$$

Bloch condition

$$\psi(z + d) = e^{ikd}\psi(z)$$

$$2\cos kd = 2\cos\frac{\omega d}{c}\frac{a|n_1| - b|n_2|}{d} - \left(\frac{Z_1}{Z_2}\frac{n_1}{|n_1|}\frac{|n_2|}{n_2} + \frac{Z_2}{Z_1}\frac{|n_1|}{n_1}\frac{n_2}{|n_2|} + 2\right) \times \sin\frac{a\omega|n_1|}{c}\sin\frac{b\omega|n_2|}{c}$$

$$\psi(z+d) = e^{iqd}\psi(z)$$

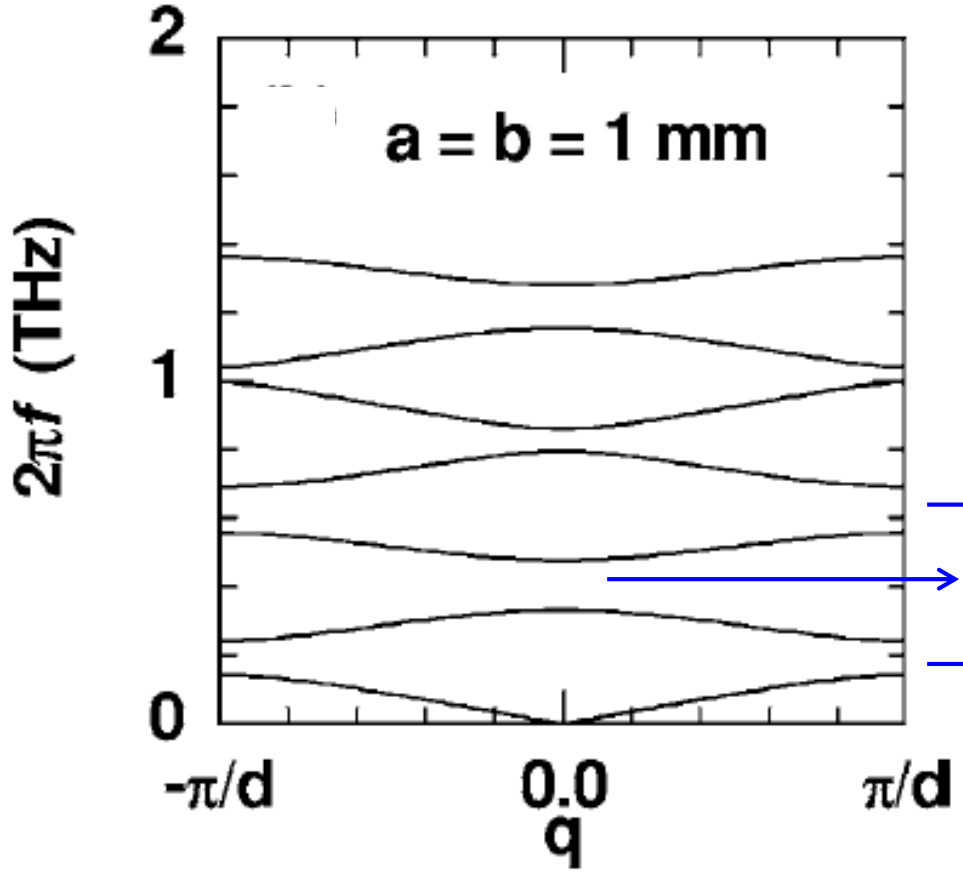

Bragg gap

Bragg gap

Bragg gap

FIG. 1. Photonic band structure ω vs q, with $\omega=2\pi f$, of a superlattice (period d) with equal alternate layers of air (with thickness a) and GaAs (thickness b and refractive index $n_2=\sqrt{\epsilon_2}\simeq 3.6$).

q is chosen within the first Brillouin zone (BZ)

$$-\pi/d \leqslant q \leqslant \pi/d$$

<n> = 0 non-Bragg gap

1D heterostruture with metamaterials

$$\langle n(\omega_0)\rangle = \frac{1}{d}\int_0^d n(z,\omega_0)dz = \frac{an_1 - b|n_2(\omega_0)|}{d} = 0$$

$$|n_2(\omega_0)| = \frac{a}{b}n_1$$

<n> = 0 gap

bandwidth around ω_0

<n> = 0 non-Bragg gap

1 D heterostruture with metamaterials

Yu Yuang et al, Optics Express 14, 2220 (2006)
Experimental verification of zero order bandgap in a layered stack of left-handed and right-handed materials

L. Zhang et al, J. Phys. D: Appl. Phys. 40, 2579-2583 (2007)
Zero-n gaps of photonic crystals consisting of positive and negative index materials in microstrip transmission lines

S. Kocaman et al, PRL 102, 203905 (2009)
Observation of zeroth-order band gaps in negative-refraction photonic crystal superlattices at near-infrared frequencies

<n> = 0 gap
a bandwidth around $\omega_0 = 2\pi\nu_0$

a non-Bragg gap

robustness with respect to the layer size:
not a Bragg gap

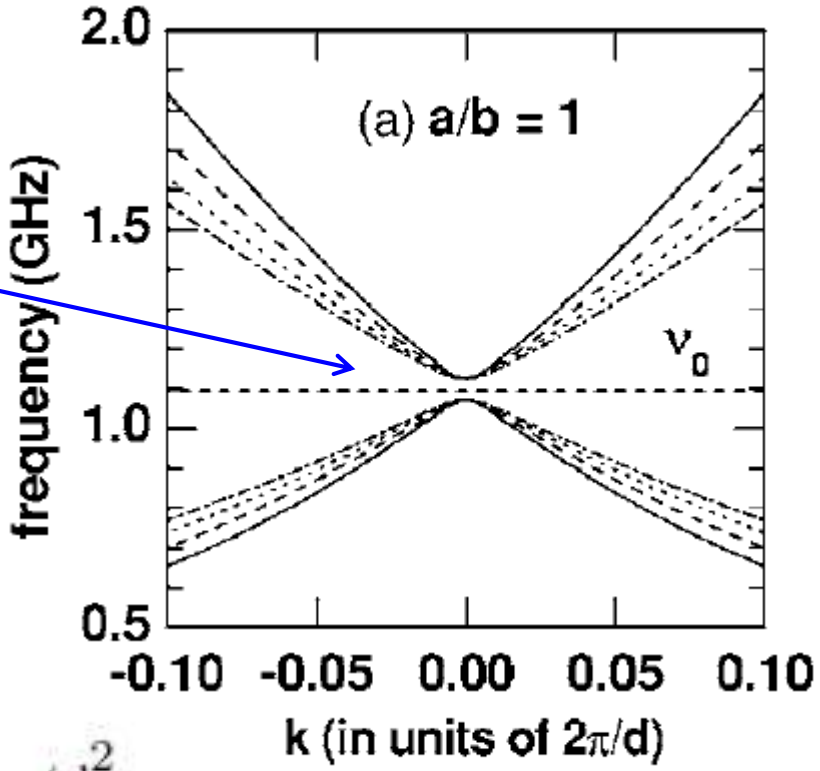

$$\varepsilon_B(\omega) = \varepsilon_0 - \frac{\omega_e^2}{\omega^2} \; ; \; \mu_B(\omega) = \mu_0 - \frac{\omega_m^2}{\omega^2}$$

$\nu_0 = 1.1$ GHz

$\omega_e^2 = \omega_m^2 = 100$; $\varepsilon_0 = 1.21$; $\mu_0 = 1.0$

with ω in GHz

solid	*a* = 12 *mm*
dash	a = 14 mm
dotted	a = 16 mm
dash-dotted	*a* = 18 *mm*

S. B. Cavalcanti, M. de Dios-Leyva, E. Reyes-Gómez, and L. E. Oliveira
Phys. Rev. E 75, 026607 (2007)

Plasmon polaritons in photonic superlattices containing a left-handed material

oblique incidence

E. Reyes-Gómez, D. Mogilevtsev, S. B. Cavalcanti, C. A. A. de Carvalho and L. E. Oliveira

EPL, **88** (2009) 24002

$\varepsilon(z) = \varepsilon(z+d);\ \mu(z) = \mu(z+d)$

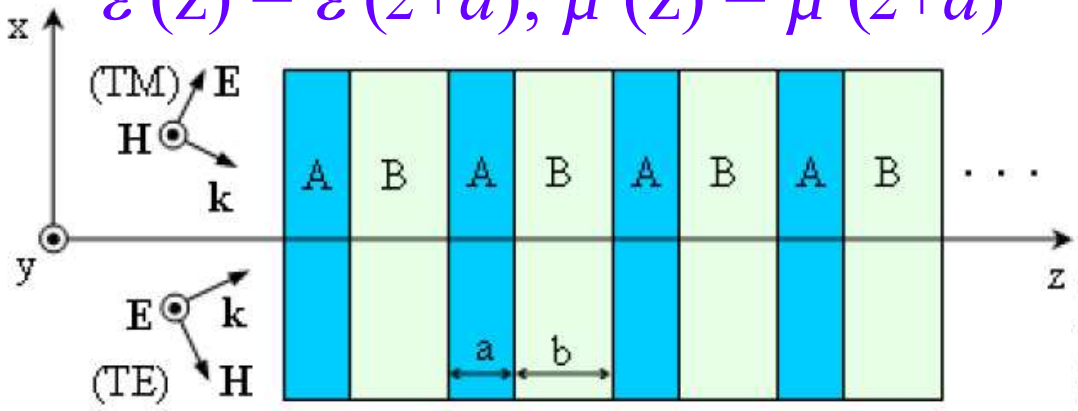

Fig. 1: (Color online) Pictorial view of the 1D multilayer photonic superlattice with layers A and B in periodic arrangement, and the electric and magnetic fields for the TE-like and TM-like electromagnetic waves schematically shown. Note that, for normal incidence, the two polarizations are equivalent.

layers A of air

$$\epsilon_B(\omega) = \epsilon_0 - \frac{\omega_e^2}{\omega^2}$$

$$\mu_B(\omega) = \mu_0 - \frac{\omega_m^2}{\omega^2}$$

where $\epsilon_B(\omega)$ and $\mu_B(\omega)$ are the dielectric permittivity and magnetic permeability in slab B, respectively, one may choose [10,11] $\epsilon_0 = 1.21$ and $\mu_0 = 1.0$, and the electric/magnetic plasmon modes are at $\nu = \nu_e = \frac{\omega_e}{2\pi\sqrt{\epsilon_0}}$ and $\nu = \nu_m = \frac{\omega_m}{2\pi\sqrt{\mu_0}}$, which correspond to the solutions of $\epsilon_B(\omega) = 0$ and $\mu_B(\omega) = 0$, respectively.

plasmons can couple with photons to create plasmon-polariton quasiparticles

longitudinal bulk-like plasmon polaritons

layers A of air $\varepsilon_A = \mu_A = 1$

B: Dispersive Metamaterials

$$\varepsilon_B(\omega) = \varepsilon_0 - \frac{\omega_e^2}{\omega^2}, \quad \mu_B(\omega) = \mu_0 - \frac{\omega_m^2}{\omega^2}$$

$\epsilon_0 = 1.21$ and $\mu_0 = 1.0$
$\omega_e/2\pi = \omega_m/2\pi = 3\,\mathrm{GHz}$

G. V. Eleftheriades, A. K. Yyer, and P. C. Kremer, IEEE Trans. Microwave Theory Tech. 50, 2702 (2002); A. Grbic and G. V. Eleftheriades, JAP 92, 5930 (2002); L. Liu et al, JAP 92, 5560 (2002)

Plasmonic modes

$$\epsilon_B(\omega) = 0 \qquad \mu_B(\omega) = 0$$

$$\omega = \bar{\omega}_e = \frac{\omega_e}{\sqrt{\epsilon_0}} \qquad \omega = \bar{\omega}_m = \frac{\omega_m}{\sqrt{\mu_0}}$$

J. A. Monsoriu et al, Opt. Express. 14, 12958 (2006); R. A. Depine et al, Phys. Lett. A 364, 352 (2007); S. K. Singh et al, Sol. State Commun. 143, 217 (2007); E. R. Gómez et al, Europhys. Lett. 88, 24002/1-6 (2009), C. A. A. de Carvalho, S. B. Cavalcanti, E. Reyes-Gómez, and L. E. Oliveira, Phys. Rev. B 83, 081408(R) (2011)

pure photonic modes

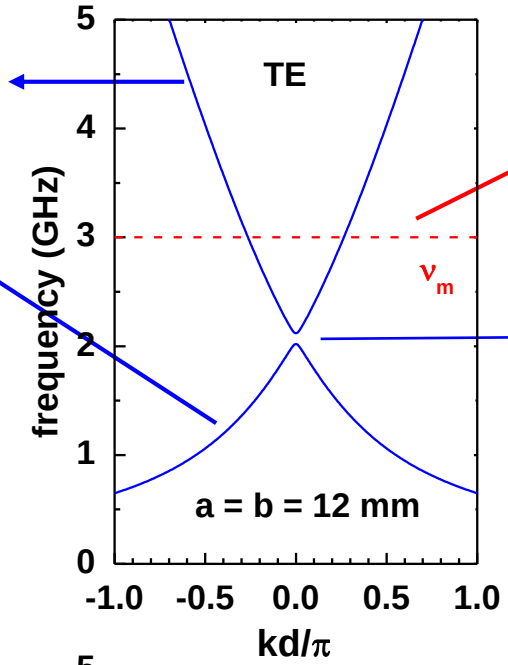

pure plasmon mode

$$\nu = \nu_m = \frac{\omega_m}{2\pi\sqrt{\mu_0}}$$

<n> = 0

non-Bragg gap

θ = 0

plasmon-polariton (PP) modes

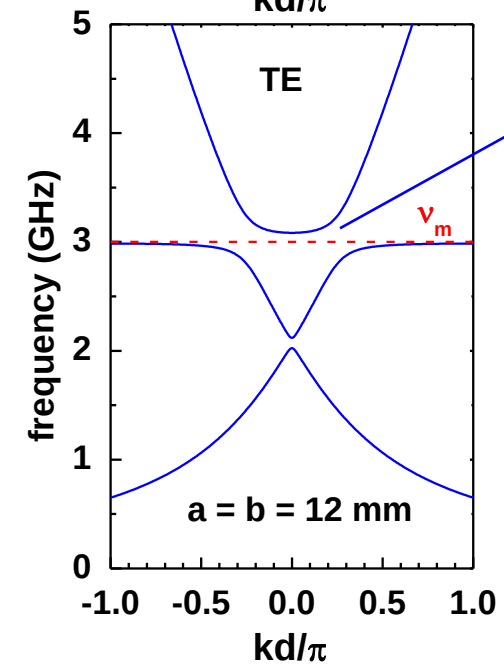

plasmon-polariton non-Bragg gap

θ = π/12

E. R. Gómez et al, Europhys. Lett. 88, 24002/1-6 (2009)

plasmon-polariton (PP) gap

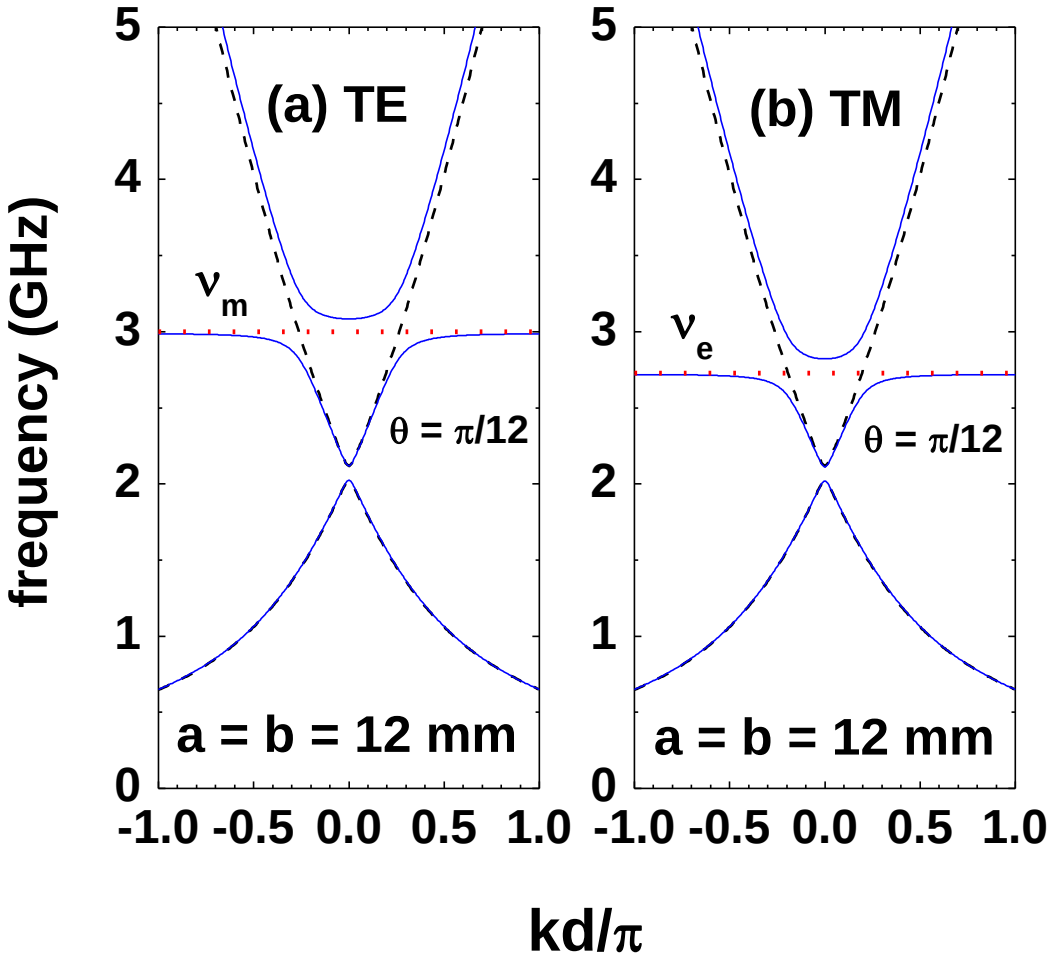

Dotted lines indicate the pure electric/magnetic plasmon modes at $\nu = \nu_e = \frac{\omega_e}{2\pi\sqrt{\epsilon_0}}$ and $\nu = \nu_m = \frac{\omega_m}{2\pi\sqrt{\mu_0}}$. Solid and dashed lines correspond to $\theta = \pi/12$ and $\theta = 0$ incidence angles, respectively.

$\epsilon_0 = 1.21$ and $\mu_0 = 1.0$

$\omega_e/2\pi = \omega_m/2\pi = 3\,\mathrm{GHz}$

E. R. Gómez, D. Mogilevtsev, S. B. Cavalcanti, C. A. A. de Carvalho, and L. E. Oliveira, Europhys. Lett. 88, 24002 (2009)

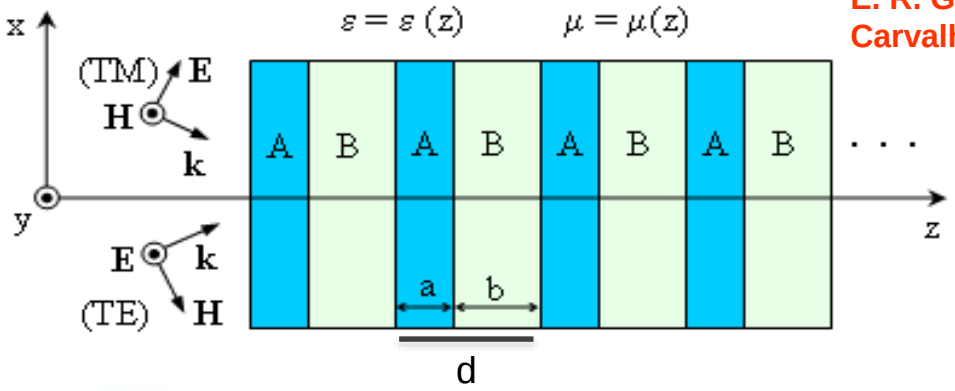

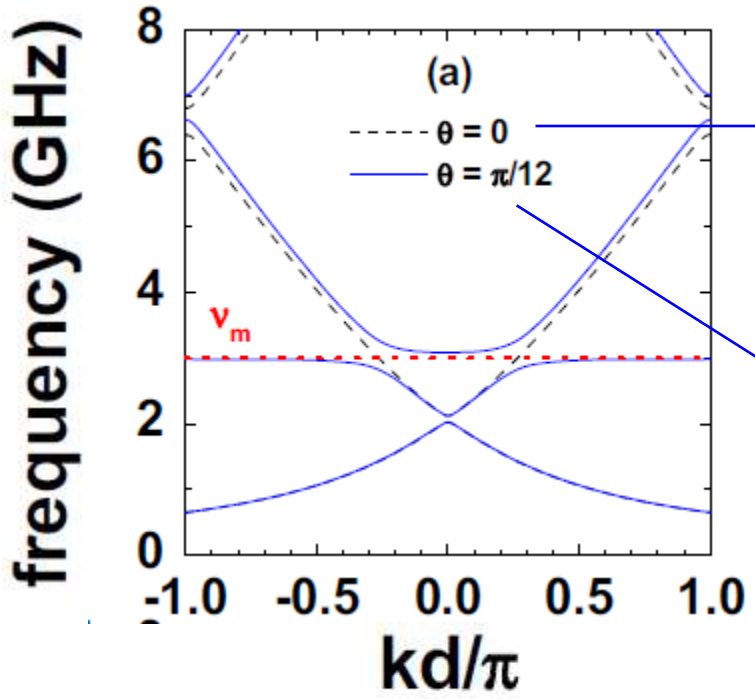

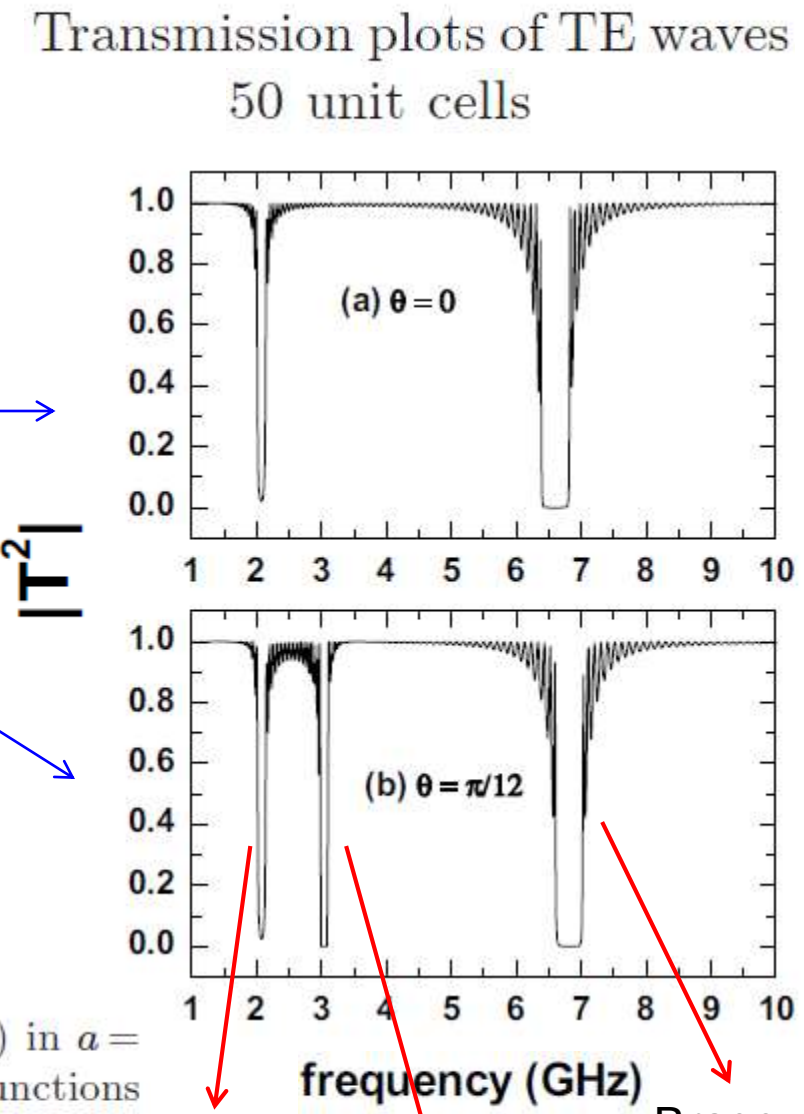

Fig. 3: (Color online) TE dispersion relations $\nu = \nu(k)$ in $a = b = 12$ mm photonic periodic superlattices ($\nu = \frac{\omega}{2\pi}$) as functions of various incidence angles. Here, dotted lines indicate the pure magnetic plasmon modes at $\nu = \nu_m = \frac{\omega_m}{2\pi\sqrt{\mu_0}}$. Dashed lines correspond to $\theta = 0$ and solid lines correspond to (a) $\theta = \pi/12$,

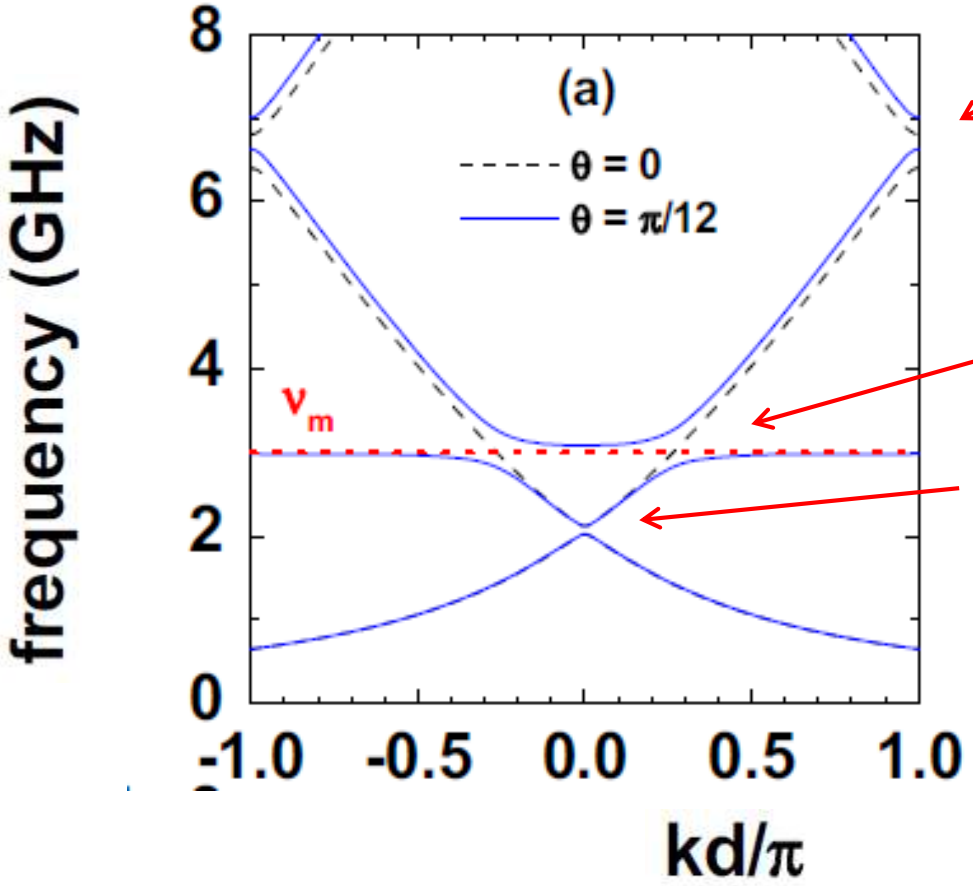

Bragg-gap

Plasmon-polariton gap

Zero *n*-gap

Sir J. Pendry, 7 April 2003

Vol. 11, No. 7,

OPTICS EXPRESS 639

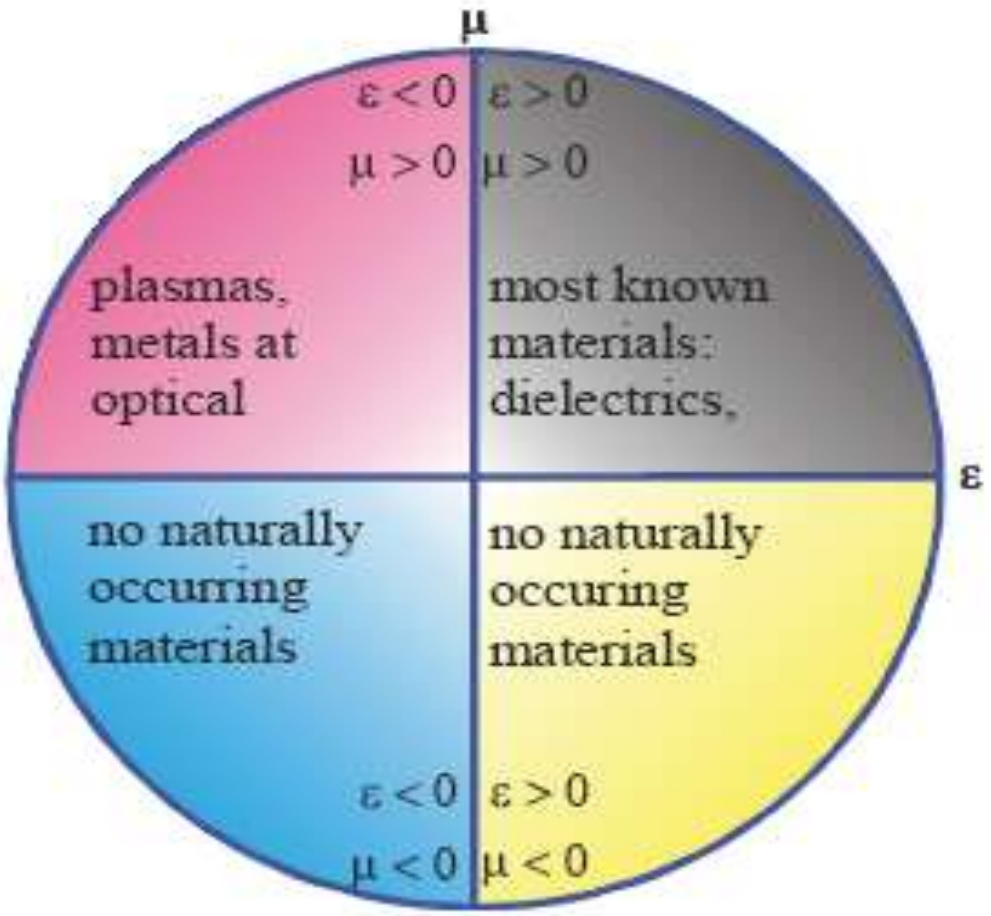

Fig. 2. Parameter space for ε, μ .

PHYSICAL REVIEW D 93, 105005 (2016)

Relativistic electron gas: A candidate for nature's left-handed materials

C. A. A. de Carvalho

Not found? Relativity to the rescue!

Nonrelativistic physics: v/c<<1, magnetic responses suppressed.

Relativistic physics: v/c ≈ 1, magnetic and electric fields interchangeable by a Lorentz transformation.

A simple system to investigate: the relativistic electron gas. Its nonrelativistic limit admits negative permittivity.

We, thus, resort (historical justice) to **QED at finite temperature & density** to profit from its symmetries.

PHYSICAL REVIEW D 93, 105005 (2016)

Relativistic electron gas: A candidate for nature's left-handed materials

C. A. A. de Carvalho
Instituto de Física, Universidade Federal do Rio de Janeiro—UFRJ

The electric permittivities and magnetic permeabilities for a relativistic electron gas are calculated from quantum electrodynamics at finite temperature and density as functions of temperature, chemical potential, frequency, and wave vector. The polarization and the magnetization depend linearly on both electric and magnetic fields, and are the sum of a zero-temperature and zero-density vacuum part with a temperature- and chemical-potential-dependent medium part. Analytic calculations lead to generalized expressions that depend on three scalar functions. In the nonrelativistic limit, results reproduce the Lindhard formula. In the relativistic case, and in the long wavelength limit, we obtain the following: (i) for $\omega = 0$, generalized susceptibilities that reduce to known nonrelativistic limits; (ii) for $\omega \neq 0$, Drude-type responses at zero temperature. The latter implies that both the electric permittivity ϵ and the magnetic permeability μ may be simultaneously negative, a behavior characteristic of metamaterials. This unambiguously indicates that the relativistic electron gas is one of nature's candidates for the realization of a negative index of refraction system. Moreover, Maxwell's equations in the medium yield the dispersion relation and the index of refraction of the electron gas. Present results should be relevant for plasma physics, astrophysical observations, synchrotrons, and other environments with fast-moving electrons.

relativistic $T = 0$ results can be tested is in a synchrotron accelerator. The electrons inside the beam are relativistic and well separated (which favors an independent particle approximation), and one can actually probe the electromagnetic responses of the beam to externally applied time-dependent fields by monitoring the fields inside the beam. In astrophysical scenarios, relativistic electron gases do occur [15], and their electromagnetic responses may be probed by comparing incident and scattered radiation. Finally, temperature effects may be tested in relativistic electron gases ejected from stars.

[15] L. A. N. da Costa, Astron. Astrophys. **70**, 477 (1978).

Down memory lane: Lindhard

$$\varepsilon_L(\vec{q},\omega) = 1 - \frac{4\pi e^2}{q^2}\int \frac{d\vec{k}}{4\pi^3}\frac{f(\varepsilon_{\vec{k}+\vec{q}}) - f(\varepsilon_{\vec{k}})}{\varepsilon_{\vec{k}+\vec{q}} - \varepsilon_{\vec{k}} - \hbar\omega - i\hbar\eta}$$

The above result was first obtained by LINDHARD and later by NOZIÈRES and PINES, who used a many-body procedure in the so-called RANDOM-PHASE APPROXIMATION (RPA) for a Fermi gas. It is restricted to LINEAR RESPONSE.

Drude & Thomas-Fermi limits

One may show that the Lindhard dielectric function reduces to the Drude result, when k → 0

$$\varepsilon_{Drude}(\vec{k} \to 0, \omega) = 1 - \frac{\omega_p^2}{\omega^2}$$

Moreover, when k → 0 and ω = 0, the Lindhard dielectric function reduces to the one obtained by the so-called Thomas-Fermi screening:

$$\varepsilon_{TF}(\vec{k}, \omega = 0) = 1 + \frac{k_{TF}^2}{k^2}$$

$$\text{with } k_{TF}^2 = \frac{4me^2 k_F}{\pi \hbar^2}$$

Quantum electrodynamics (QED)

$$\mathcal{L} = -\frac{1}{4} F_{\mu\nu} F^{\mu\nu} + \bar{\psi}(i\gamma.\partial - m)\psi - e\bar{\psi}\gamma^{\mu} A_{\mu}\psi$$

$$F_{\mu\nu} = \partial_{\mu} A_{\nu} - \partial_{\nu} A_{\mu} \qquad j_{\mu} = e\bar{\psi}\gamma_{\mu}\psi$$

$$\mathcal{L} = -\frac{1}{4} F_{\mu\nu} F^{\mu\nu} + \bar{\psi}(i\gamma.D - m)\psi$$

Describes quantized electrons and photons in interaction.

The partition function

$$Z = \mathrm{Tr}\, e^{-\beta(\hat{H} - \xi \Delta \hat{N})}$$

$$\Delta N = N_e - N_p$$

In terms of path integrals over the fields A & ψ,

$$Z = \oint [d\Omega]\, \delta(\mathcal{G}) e^{-S_A[A]} Z_e[A]$$

$$Z_e[A] = \oint [i d\psi^\dagger][d\psi] e^{-S_e[\psi^\dagger, \psi, A]}$$

V. Popov, Functional Methods in Condensed Matter Theory

Finite temperature & density

Euclidean space, boundary conditions, fixed ΔN.

$$A_\nu(0,\vec{x}) = A_\nu(\beta,\vec{x})$$
$$\psi(0,\vec{x}) = -\psi(\beta,\vec{x})$$

$$\mathcal{L}_e = \bar{\psi}\Gamma_A\psi$$

$$\Gamma_A = G_A^{-1} = i\gamma.D - m - i\xi\gamma_4$$

Finite-Temperature Field Theory, **J.I. Kapusta & C. Gale, Cambridge University Press, 2006**

Dirac sea & Fermi band

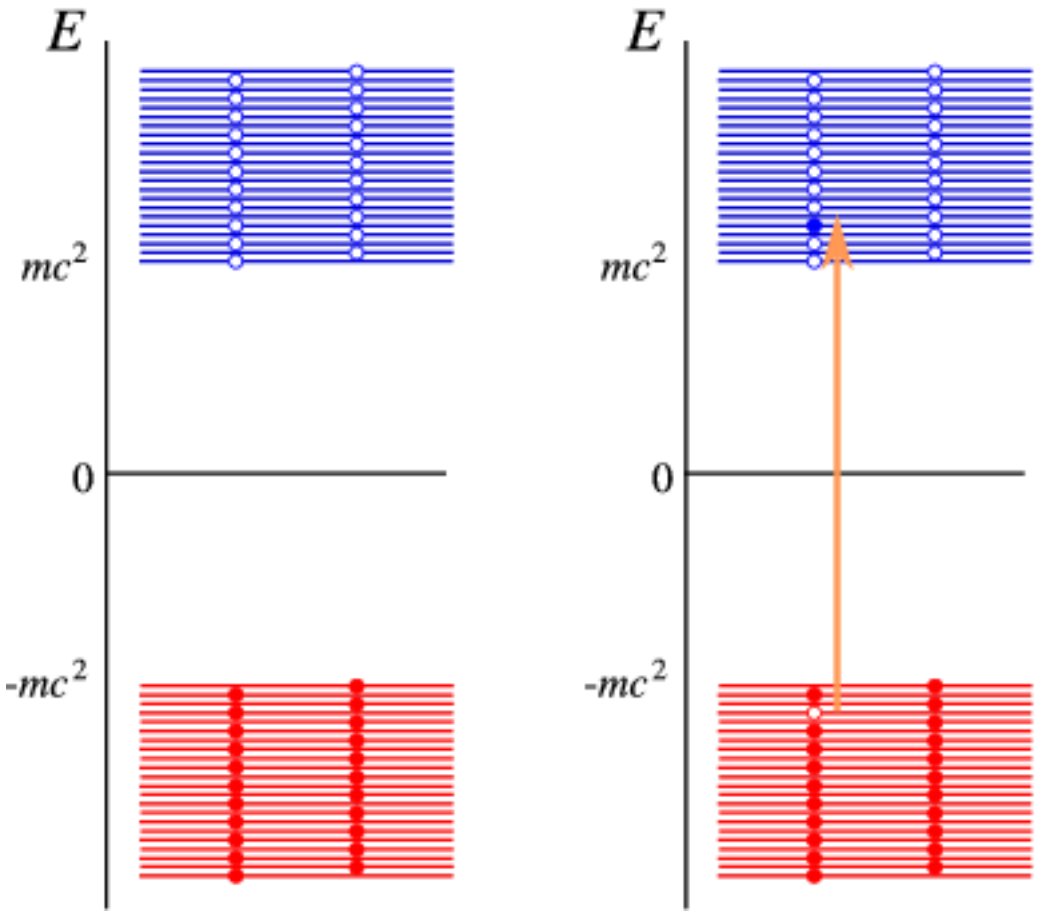

oer.physics.manchester.ac.uk

The semiclassical expansion

$$A_\mu = A_\mu^{(c)} + \hbar a_\mu$$

1. **Expand action in the classical (external) field, integrate over aμ.**
2. **Keep only O(α), neglect the O(α^2) e-e interactions.**
3. **Integrate over the electron field, neglect nonlinear terms O(α[αE^2/m^4], α[αB^2/m^4]) (linear response).**
4. **Extremize resulting effective action to derive equations of motion for E & B.**
5. **Extract electromagnetic (EM) responses from those equations.**

The polarization tensor

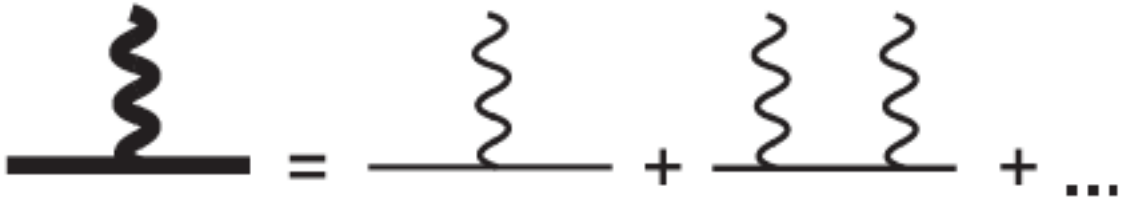

$$iq_\mu \tilde{P}_{\mu\nu}(q) = \tilde{\Pi}_{\nu\sigma}(q)\tilde{A}_\sigma(q)$$

$$\tilde{\Pi}_{\nu\sigma} = -\frac{e^2}{\beta}\sum_{n=-\infty}^{+\infty}\int \frac{d^3p}{(2\pi)^3}\mathrm{Sp}[\gamma_\nu G_0(p)\gamma_\sigma G_0(p-q)]$$

$$\tilde{P}_{\mu\nu} = \frac{\tilde{\Pi}_{\mu\sigma}}{q^2}F_{\nu\sigma} - \frac{\tilde{\Pi}_{\nu\sigma}}{q^2}F_{\mu\sigma}$$

Vacuum & Medium

$$\tilde{\Pi}_{\nu\sigma} = \tilde{\Pi}^{(v)}_{\nu\sigma} + \tilde{\Pi}^{(m)}_{\nu\sigma}$$

I. A. Akhiezer & S. V. Peletminskii, Sov. Phys. JETP 11, 1316 (1960)

$$\mathcal{A} = \frac{-e^2}{2\pi^3 q^2}\mathrm{Re}\int \frac{d^3p}{\omega_p} n_F(p) \frac{p.(p+q)}{q^2 - 2p.q} + (1 - \frac{3q^2}{2|\vec{q}|^2})\mathcal{B}$$

$$\mathcal{B} = \frac{-e^2}{2\pi^3 q^2}\mathrm{Re}\int \frac{d^3p}{\omega_p} n_F(p) \frac{p.q - 2p_4(q_4 - p_4)}{q^2 - 2p.q}$$

Later on, quantities with asterisks have $q_4 = i\,\omega + \eta$

Constitutive equations I

$$H_{\mu\nu} = F_{\mu\nu} + P_{\mu\nu}$$

$$H_{4j} = iD^j$$

$$H_{ij} = \epsilon_{ijk} H^k$$

$$\vec{D} = \vec{E} + \vec{P}$$

$$\vec{H} = \vec{B} - \vec{M}$$

Constitutive equations II

$$\tilde{D}^j = \epsilon^{jk}\tilde{E}^k + \tau^{jk}\tilde{B}^k$$

$$\tilde{H}^j = (\mu^{-1})^{jk}\tilde{B}^k + \sigma^{jk}\tilde{E}^k$$

$$\epsilon^{jk} = \epsilon\delta^{jk} + \epsilon'\hat{q}^j\hat{q}^k$$

$$(\mu^{-1})^{jk} = \mu^{-1}\delta^{jk} + \mu'^{-1}\hat{q}^j\hat{q}^k$$

$$\tau^{jk} = \tau\epsilon^{jkl}\hat{q}^l,\ \sigma^{jk} = \sigma\epsilon^{jkl}\hat{q}^l$$

Electromagnetic responses I

$$\epsilon = 1 + (2 - \frac{\omega^2}{q^2})\mathcal{C}^* + \mathcal{A}^* + (1 - \frac{\omega^2}{|\vec{q}|^2})\mathcal{B}^*$$

$$\mu^{-1} = 1 + (2 + \frac{|\vec{q}|^2}{q^2})\mathcal{C}^* + \mathcal{A}^* - 2\frac{\omega^2}{|\vec{q}|^2}\mathcal{B}^*$$

$$\epsilon' = -\mu'^{-1} = \frac{|\vec{q}|^2}{q^2}\mathcal{C}^* - \mathcal{A}^*$$

$$\tau = \sigma = \frac{\omega}{|\vec{q}|}(\frac{|\vec{q}|^2}{q^2}\mathcal{C}^* - \mathcal{B}^*)$$

Electromagnetic responses II

$$\mathcal{C}^* = \frac{-e^2}{12\pi^2}\{\frac{1}{3} + 2(1 + \frac{2m^2}{q^2})[h\,\mathrm{arccot}(h) - 1]\}$$

$$h = \sqrt{(4m^2/q^2) - 1}$$

$$e^2/(4\pi\hbar c) = 1/137$$

This is the usual vacuum contribution

Long wavelength Drude responses I

For any T. At T=0, analytic expressions, ζ= ξ/m.

$$\epsilon = 1 - \frac{\omega_e^2}{\omega^2} + \frac{e^2}{3\pi^2} g_e(\zeta) + O(\frac{\omega^2}{4m^2})$$

$$\frac{\omega_e^2}{4m^2} = \frac{e^2}{12\pi^2} \frac{(\zeta^2-1)^{3/2}}{\zeta}$$

$$\Omega_e^2 = \omega_e^2[1 + \frac{e^2}{3\pi^2} g_e(\zeta)]^{-1} \simeq \omega_e^2$$

Long wavelength Drude responses II

$$\mu^{-1} = 1 - \frac{\omega_m^2}{\omega^2} - \frac{5e^2}{6\pi^2}\, g_m(\zeta) + O(\frac{\omega^2}{4m^2})$$

$$\frac{\omega_m^2}{4m^2} = \frac{2e^2}{12\pi^2}\frac{(\zeta^2-1)^{3/2}}{\zeta}$$

Drude behavior for the inverse of μ.
Both responses negative at low frequencies.

Negative index of refraction

$$q_\mu \tilde{H}_{\mu\nu} = 0 \qquad \epsilon_{\mu\nu\alpha\beta} q_\nu \tilde{F}_{\alpha\beta} = 0$$

$$[(\mu^{-1} + \frac{\omega}{|\vec{q}|}\sigma)|\vec{q}|^2 - (\epsilon - \frac{|\vec{q}|}{\omega}\tau)\omega^2]\tilde{E}_i = 0$$

$$[(\mu^{-1} + \frac{\omega}{|\vec{q}|}\sigma)|\vec{q}|^2 - (\epsilon - \frac{|\vec{q}|}{\omega}\tau)\omega^2]\tilde{B}_i = 0$$

$$|\vec{q}|^2 - (\mu\epsilon)\,\omega^2 + 2(\mu\tau)\,\omega|\vec{q}| = 0$$

For long wavelengths, the last term vanishes.

EPL, 114 (2016) 17009

The electromagnetic response of a relativistic Fermi gas at finite temperatures: Applications to condensed-matter systems

E. Reyes-Gómez[1], L. E. Oliveira[2] and C. A. A. de Carvalho[3,4]

[1]*Instituto de Física, Universidad de Antioquia UdeA - Calle 70 No. 52-21, Medellín, Colombia*
[2]*Instituto de Física, Universidade Estadual de Campinas-Unicamp - Campinas-SP, 13083-859, Brazil*
[3]*Instituto de Física, Universidade Federal do Rio de Janeiro-UFRJ - Rio de Janeiro-RJ, 21945-972, Brazil*
[4]*Inmetro, Campus de Xerém - Duque de Caxias-RJ, 25250-020, Brazil*

received on 12 April 2016; accepted by B. A. van Tiggelen on 24 April 2016

Abstract – We investigate the electromagnetic response of a relativistic Fermi gas at finite temperatures. Our theoretical results are first-order in the fine-structure constant. The electromagnetic permittivity and permeability are introduced via general constitutive relations in reciprocal space, and computed for different values of the gas density and temperature. As expected, the electric permittivity of the relativistic Fermi gas is found in good agreement with the Lindhard dielectric function in the low-temperature limit. Applications to condensed-matter physics are briefly discussed. In particular, theoretical results are in good agreement with experimental measurements of the plasmon energy in graphite and tin oxide, as functions of both the temperature and wave vector. We stress that the present electromagnetic response of a relativistic Fermi gas at finite temperatures could be of potential interest in future plasmonic and photonic investigations.

Electric permittivities & Lindhard

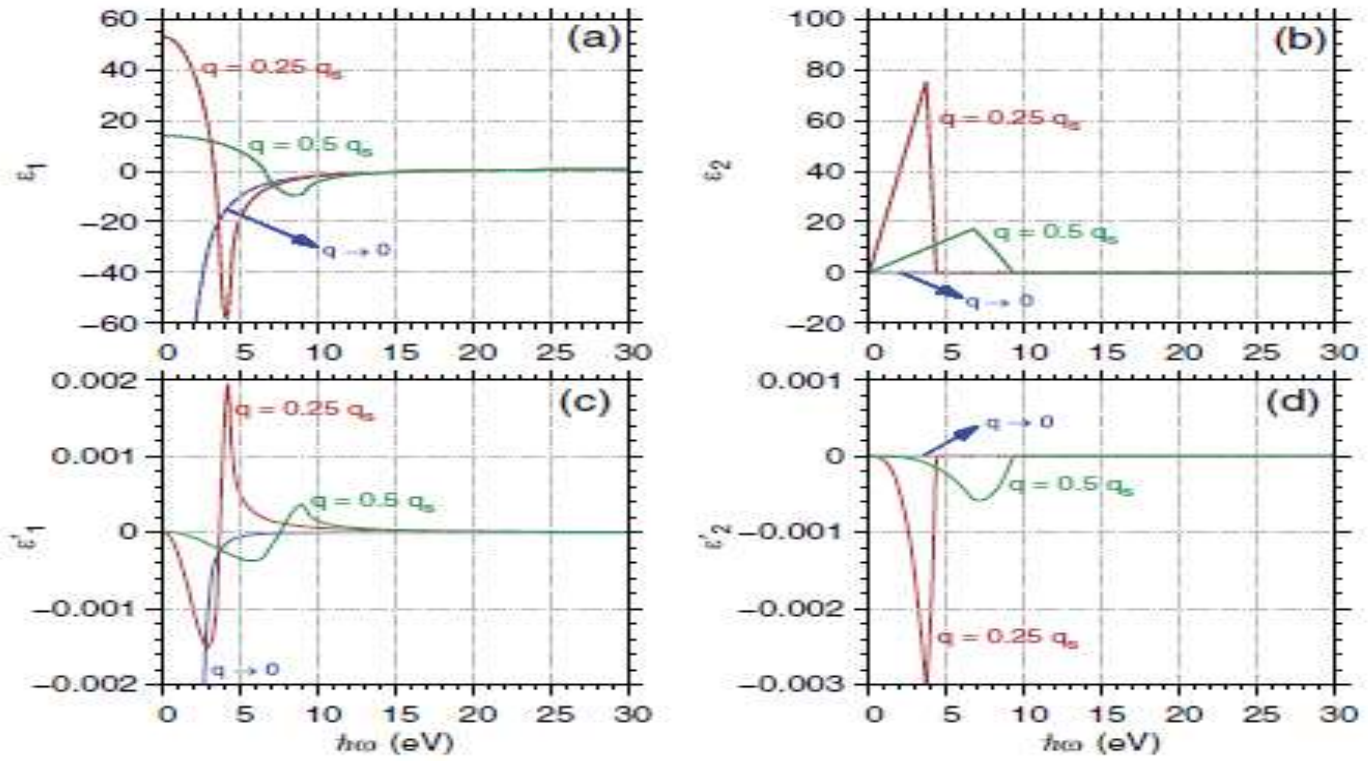

Fig. 1: (Color online) Real and imaginary parts of ε and ε' as functions of $\hbar\omega$. Calculations were performed for various values of q in units of q_s (see text) and for η corresponding to the electron density in a primitive cell of a silicon crystal. Solid and dashed lines correspond to the present theoretical results (cf. eqs. (6) and (7)) at $T = 5$ K and to the Lindhard dielectric function [3,4], respectively.

Plasmon frequencies for graphite

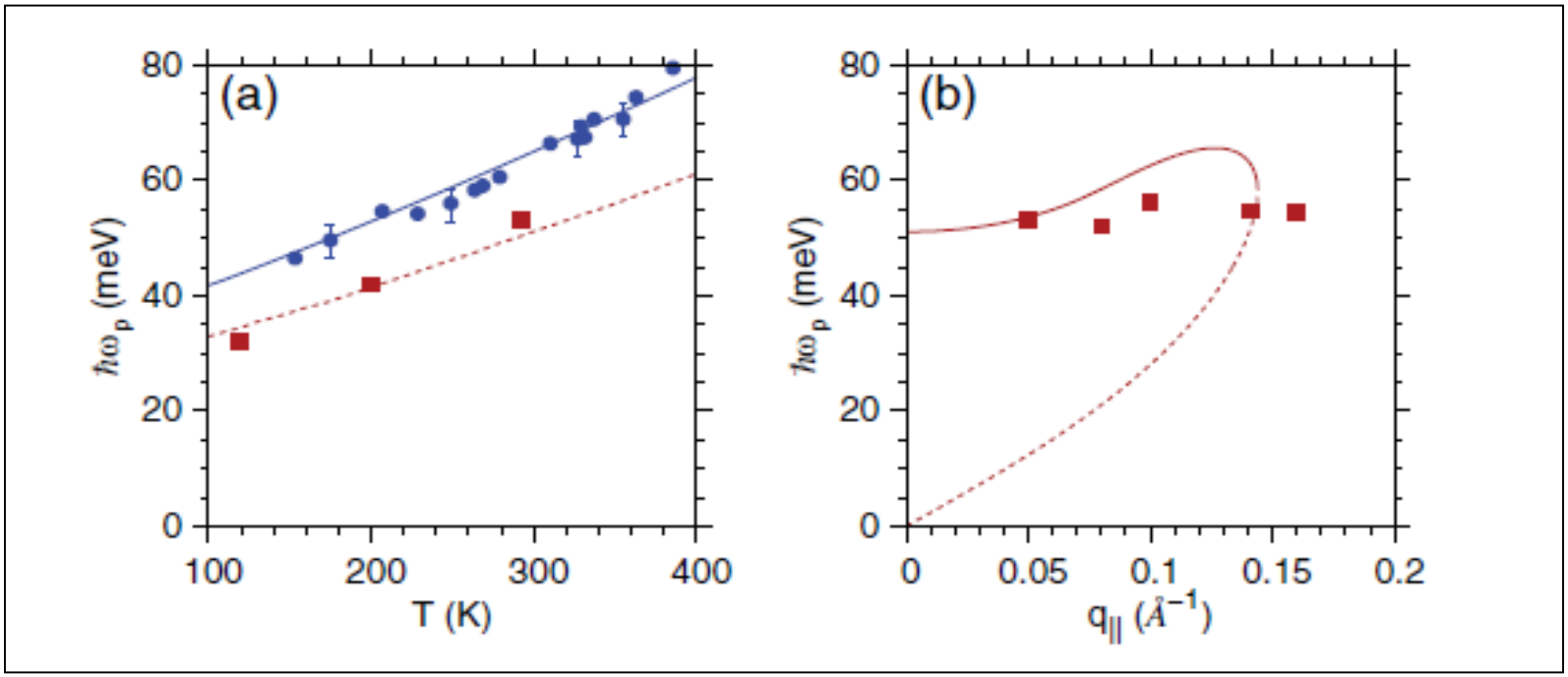

Plasmon frequencies for graphite as a function of temperature and wavenumber, compared to experimental results obtained by Jensen et al and Portail et al. Full references in the article in EPL.

Plasmon frequencies for tin oxide

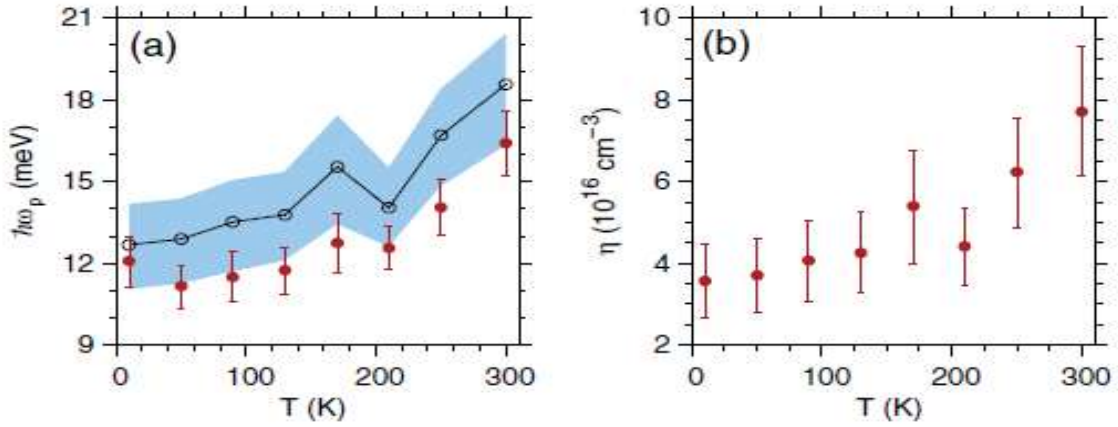

Fig. 3: (Color online) (a) Plasmon energy of tin oxide nanowire films as a function of the T temperature. Solid circles correspond to experimental measurements by Zou *et al.* [10]. Open circles correspond to numerical results obtained from eq. (6) by using the carrier density, at each value of T, reported by Zou *et al.* [10] (see panel (b)). Calculations were performed in the limit $q \to 0$ by replacing the free-electron mass by the $m_c^* = 0.31\, m$ conduction-effective mass of tin oxide [10]. The solid line connecting open circles is a guide to the eye. The dark area corresponds to the uncertainty interval of the calculated plasmon energy at each value of T and was computed by propagating the error of the carrier density estimated by the error bars in panel (b).

Negative refraction of electrons spotted in graphene

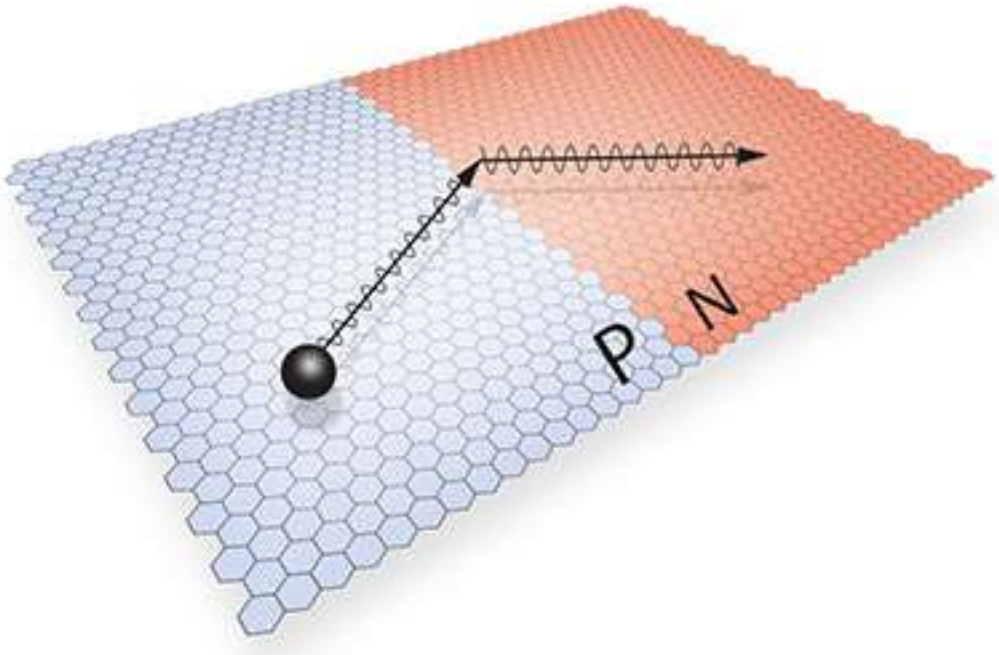

Wrong way: electrons undergoing negative refraction at a p–n junction
S. Chen at al, Science 30, 353/6307, pp 1522-1525 (2016)

Imaginary parts of responses at T=0

(D.M. Reis)

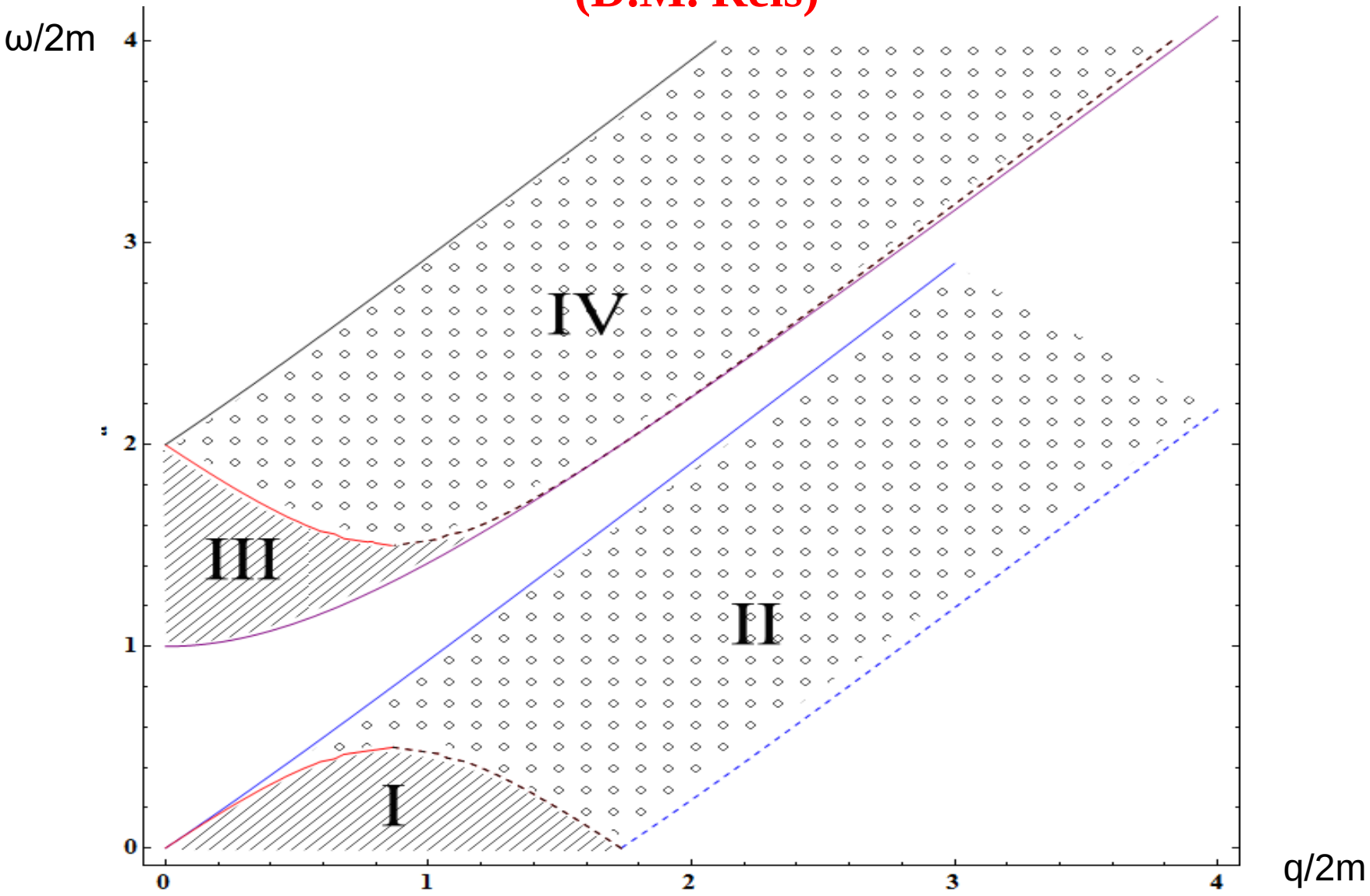

Conclusions

The relativistic electron gas exhibits rich EM responses: metamaterial behavior, plasmons, imaginary parts.

QED at finite temperature & density uses symmetry, and gives both vacuum and medium contributions.

Physical scenarios involving relativistic electron gases such as synchrotrons and astrophysical situations are natural experimental testing grounds.

Connection with relativistic plasmons and calculations for relativistic Bose gases (condensates) will appear in the near future.

A física, com seu método científico, tornou-se um paradigma para todas as ciências naturais e esteve na origem da revolução tecnológica do final do século XX. Sua importância política e socioeconômica teve reconhecimento universal naquele século. Nos países industrializados, físicos passaram a participar de comissões governamentais em que se definiam políticas para a sociedade graças ao impacto de sua ciência na vida do planeta. Não há como negar que o poderio nuclear, a guerra eletrônica, o hardware da sociedade da informação e outros condicionantes da geopolítica mundial refletem claramente esse impacto.

Essa ciência tão rica, cuja missão é tão intimamente ligada à saga da humanidade rumo ao conhecimento do mundo ao seu redor, inicia o milênio acreditando saber contar a história do universo desde 10^{-43} s até sua idade atual, estimada em 13,7 x 10^{9} anos (~10^{17} s), uma história que envolve pelo menos 50 bilhões de galáxias distribuídas em gigantescos filamentos que se alternam com imensos vazios. Dos megaparsecs da astrofísica, aos 10^{-17}cm investigados pelos aceleradores de partículas, a física observa, detecta e mede com precisão cada vez maior, teoriza com ousadia, a ponto de abrir novas áreas na matemática, e se aventura rumo a sistemas cada vez mais complexos, embarcando integralmente na multidisciplinaridade que há de ser a marca registrada do novo milênio.

Carlos Alberto Aragão de Carvalho Fº / 2005

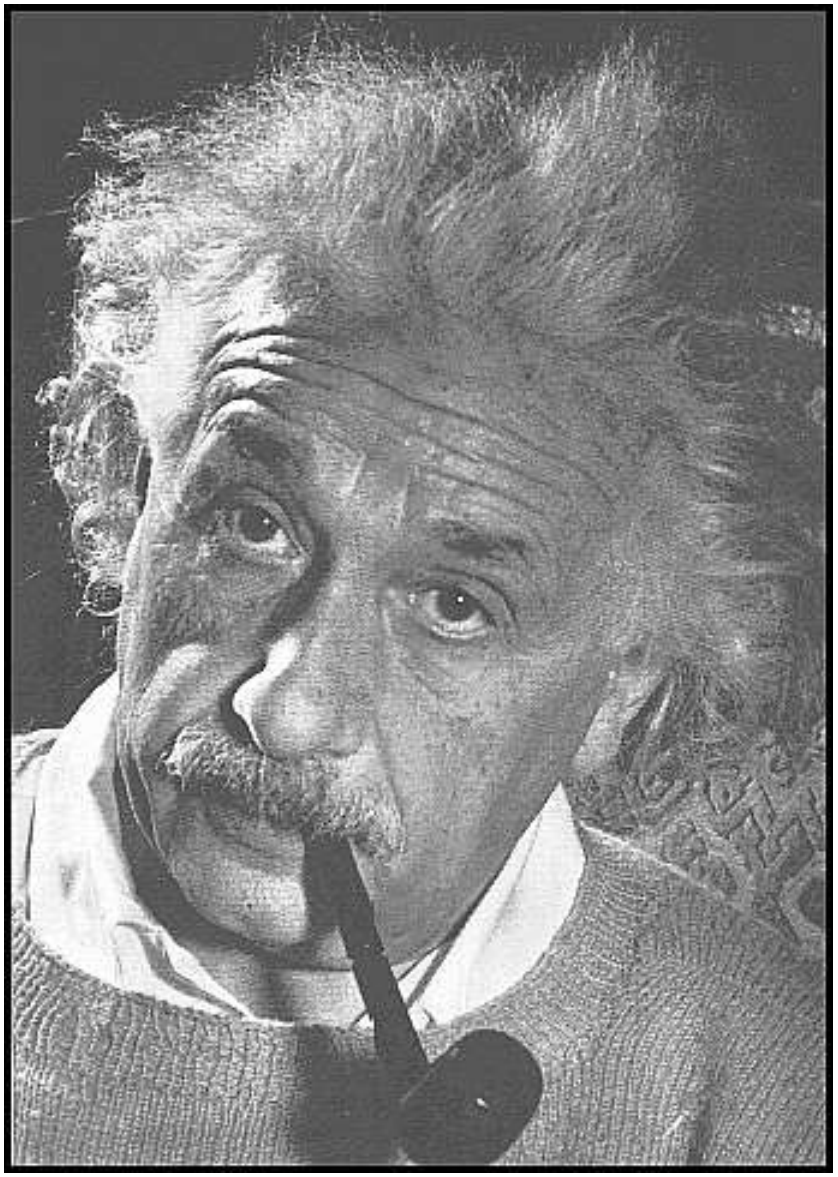

The eternal mystery of the world

is its comprehensibility

Albert Einstein

Physicist

Collaborators:

Collaborators for the first part of the work (plasmon-polaritons)

S. B. Cavalcanti
UFAL, Maceió, Brazil

Alexys Bruno Alfonso
UNESP, Bauru, Brazil

Dmitri Mogilevtsev
NASB, Minsk, Belarus

Collaborators

Ernesto Reyes-Gómez
U. de Antioquia

Daniel Medeiros Reis
CBPF

Luiz Eduardo Oliveira
Unicamp

Parabéns à EPGF/UERJ! 20 anos!

carlos.aragao51@gmail.com